CONDITION ASSESSMENT OF TREATED-TIMBER GUARDRAIL POSTS

Final Report
October 2010

Sponsored by:
Wisconsin Department of Transportation

Forest Products Laboratory – U.S. Forest Service, U.S. Dept. of Agriculture
One Gifford Pinchot Drive, Madison, Wisconsin 53726-2398
Promoting healthy forests and forest-based economies through the efficient, sustainable use of our wood resources.

This page intentionally left blank.

CONDITION ASSESSMENT OF TREATED-TIMBER GUARDRAIL POSTS

Final Report
October 2010

Principal Investigator:

James P. Wacker, Research Engineer
Forest Products Laboratory
U.S. Forest Service, U.S. Department of Agriculture

Co-Principal Investigators:

David E. Kretschmann, Research Engineer
Xiping Wang, Research Forest Products Technologist
Douglas R. Rammer, Research Engineer
Forest Products Laboratory
U.S. Forest Service, U.S. Department of Agriculture

Sponsored by
Wisconsin Department of Transportation
(Project No. 0092-43-03)

Forest Products Laboratory
U.S. Forest Service, U.S. Department of Agriculture
One Gifford Pinchot Drive
Madison, WI 53726-2398
Phone: 608-231-9200
Fax: 608-231-9303
www.fpl.fs.fed.us

Acknowledgements

This project was financed in part through funds provided by the Wisconsin Department of Transportation through its research management agreement with the U.S. Forest Service Forest Products Laboratory (Project 08-CO-11111133-074). We are grateful to Erik Emerson, Pete Kemp, Lynn Saeger, and Bob Lemke of the WI-DOT for assistance in selecting test sites, coordinating field testing, and project administration. The authors also recognize the valuable contributions of the following individuals. For assistance with field testing: Carlito Calil Jr. of University of Sao Paulo (Brasil), Turker Dundar of Istanbul University (Turkey), Shan Gao of Northeast Forestry University (China), and James Gilbertson of the Forest Products Laboratory (FPL). For their assistance with laboratory testing: Sara Fishwild and Tim Nelson of the FPL Engineering Mechanics and Remote Sensing Laboratory (EMRSL).

Executive Summary

New management strategies are being considered for highway guardrail systems in the State of Wisconsin. These asset management strategies have been applied for many decades to bridges and pavements, requiring bi-annual routine inspections, and have provided numerous benefits over a structure's service life. Some of the benefits include improved user safety, more pro-active maintenance efforts, more reliable replacement decisions, and greater service life.

The focus of this study was the longitudinal barrier design commonly utilized in Wisconsin consisting of a flexible steel w-beam rail, a timber offset block, and treated sawn timber posts spaced at 75 inch intervals. Since the guardrail posts have not typically been evaluated after installation, new inspection protocols were needed that were minimally-invasive, while providing a reliable indication of the structure's condition. Since the timber posts are typically embedded approximately 3-1/2 feet into the roadway shoulder, regular inspection techniques may not provide reliable data. Non-destructive techniques were investigated that were able to provide an indication of the overall integrity of the post including the embedded portion.

The objective of this study was to evaluate nondestructive inspection techniques for assessing the condition of the timber guardrail posts. Impact-echo acoustic testing was performed on a total of 40 posts obtained from two field sites in Wisconsin recently slated for replacement. The posts were impacted at the (end-grain) topside of the post using a variety of hammer devices. The resulting acoustic response signal was captured with an accelerometer also attached to topside of the post. Signal processing was performed by NI Digital Oscilloscope utilizing the Labview software package.

In-ground acoustic tests were performed in the field on embedded posts just prior to their removal from service, while Out-of-ground acoustic tests were performed several months later in the laboratory (without soil embedment) on test supports. In addition, physical and mechanical tests were performed at the Forest Products Laboratory (FPL) on the salvaged posts after removal from service. Physical testing included size, weight, knot mapping, stress wave scanning, moisture content, and specific gravity. Mechanical testing included stiffness and ultimate strengths using a cantilevered post with a fixed support testing configuration.

Impact-echo acoustic testing was also performed on a total of 40 new treated guardrail posts at the field test sites. Out-of-ground tests were performed on test supports prior to installation and in-ground tests were performed shortly after installation. These data provide a baseline of reference for future inspections using impact-echo acoustic testing protocols. Deterioration should be monitored over time using periodic inspections and will ultimately provide an estimation of an expected service life for the timber guardrail posts.

The acoustic testing were compared between the In-ground and Out-of-ground FFT frequencies for the posts removed after several years of service. The Royalton posts had a fairly strong relationship (r^2 = 0.8476) which proved the concept may be used for guardrail post inspections. Physical testing of the salvaged posts in the laboratory indicated the internal decayed regions of the posts (see appendix). Cantilevered post bending strength testing indicated average MOR values of 2,712 lb/in.^{2} for the Royalton posts and 3,161 lb/in.^{2} for the Merrimac posts.

Future work will need to focus on further development of the impact-echo acoustic technique for nondestructive evaluation of in-service guardrail posts. Automated signal processing algorithms in a hand-held computer device would provide the best solution for inspectors. The benefits of quasi-nondestructive methods, such as resistance micro-drilling,

performed near the ground line may be a reliable indicator of post condition and residual strength and should be further investigated.

This page intentionally left blank.

TABLE OF CONTENTS

This page intentionally left blank.

Figure Listing

Figure Listing, continued;

Table Listing

This page intentionally left blank.

Introduction

Guardrail systems utilizing treated timber guardrail posts are commonly used along Wisconsin highways to protect motorists from roadside hazards. These longitudinal barriers, consisting of a rectangular timber posts and flexible steel (W-beam) guardrails have been used for several decades. Southern Yellow Pine posts pressure-treated with CCA preservatives were traditionally used but the use of local species has become more popular in the past several years. The native wood species of Red pine and White pine are now the primary species being utilized for guardrail posts in the state of Wisconsin. They are pressure-treated with ACQ preservative, a relatively new copper-based treatment that does not contain Chromium compounds found in CCA.

The service life of these treated timber post guardrail systems has been estimated to be between 10-20 years. Their durability is influenced by a number of factors including the climate, soil conditions, impact damage, maintenance, drainage conditions, and sunlight exposure. Guardrail posts in northern Wisconsin could have a significantly different service life than those located in southern areas of the state. Maybe the most important factors influencing guardrail post service life is the effectiveness of the preservative treatment and the physical post conditions at the ground line. If a post is not pressure-treated properly it will not contain a protective shell of treated material to prevent decay activity. In addition, drying defects (i.e. checking) or the presence of difficult-to-treat heartwood will provide avenues for moisture intrusion and early decay activity within the untreated interior of the posts. The critical zone extends above and below the ground line by approximately 1 ft and usually is where the earliest signs of decay activity are detected.

Routine inspections are not required and are not typically performed by WIS-DOT personnel unless there is an automobile accident. Therefore, replacement decisions are based upon past experience and are rather arbitrary. Most times the condition of the guardrail system is not assessed until the roadway is scheduled for upgrade or reconstruction. However, the FHWA is urging the states to implement new management strategies regarding their transportation-related assets. These asset management strategies have been applied for many decades to bridges and pavements, requiring routine

inspections at regular intervals. Guardrail systems represent a significant asset for the states and there is a need for the development of new inspection strategies to support these efforts. These proactive management strategies will have numerous benefits over a structure's service life. Some of the benefits include improved user safety, more pro-active maintenance efforts, more reliable replacement decisions, and greater service life. There is a need to develop new inspection protocols for treated timber guardrail posts. Several techniques are available for visual inspection of the posts. However, focusing solely on the external indicators can be misleading as the internal integrity is the most important factor associated with post bending strength under impact loads. Therefore, those techniques which provide a quantitative and nondestructive evaluation (NDE) of the interior and embedded portion of the post will be further investigated. In order to be a viable option for inspectors, an inspection technique must be simple to use and produce easily-interpretable data.

Background

Unfortunately, the amount of deterioration in wood guardrail posts cannot easily be determined by visual field inspection, so many degraded posts go unnoticed by state maintenance personnel [1]. Much of the literature on highway guardrail posts focused on their dynamic performance under vehicle impact loadings. There is no known literature that applies various nondestructive techniques to timber guardrail posts.

However, several nondestructive techniques have been investigated for evaluating timber piles in-service. Chen and Kim [2] reported that dispersive wave propagation tests were found to be a promising means of evaluating the degree of hollowness in timber piles. They studied 7 installed timber piles in the field, and 2 salvaged timber piles, an acrylic cylinder and a timber post in the laboratory. The timber post measured 100mm by 100mm by 5.5m and included an array of drilled holes in order to simulated marine borer damage. The test instrumentation included two accelerometers attached to the side of the pile at exposed portion near its top. An impact hammer was used for creating signal waves and a digital oscilloscope for capturing signal data. Their data analysis was performed by two different methods: the

Fourier transform (FT) method, and the short kernel method. The short kernel method was more effective at detecting the artificial damage in the laboratory timber post evaluations. A related nondestructive testing technique for evaluating the length of embedment of timber piles is reported by Holt et al [3]. It uses a single accelerometer to measure the time between reflected wave signals and was shown to estimate the embedment length within +/- 10 percent. The so-called *Pile Integrity Test* has recently been standardized in ASTM Standard D5882 S*tandard Test Method for Low Strain Impact Integrity Testing of Deep Foundations* [4]. A thorough description of the various field techniques for evaluating embedded timber piles is provided by White et al [5]. Additional research is needed to determine if a modified nondestructive technique based on a impact-echo acoustic approach is a viable inspection tool for timber guardrail posts.

Objective & Scope

The main focus of this study was to evaluate the effectiveness of impact-echo acoustic testing as a candidate inspection protocol for treated timber guardrail posts. Twenty posts were evaluated at each guardrail field sites: one located in southern and the other in central Wisconsin. Impact-echo acoustic NDE techniques were used at both field sites and in the laboratory. Cantilevered bending tests were performed on the salvaged posts in the laboratory to determine their residual strength values. Relationships between the NDE and residual strength date sets were also studied. A secondary focus was to conduct similar acoustic testing on the new post installations in order to create baseline data to support future performance monitoring efforts.

Materials and Methods

A number of treated sawn timber guardrail posts were evaluated in three different settings for this study. First, a test section of new guardrail posts were installed on the FPL campus and allowed for the proposed nondestructive testing technique to be investigated under the outdoor climate conditions in

Madison, Wisconsin. Second, impact-echo acoustic testing was conducted at two field sites and included both new and old posts. Third, salvaged old posts from both field sites were shipped to FPL for additional nondestructive evaluations and destructive testing in the laboratory.

Guardrail Posts

Guardrail posts were Eastern white pine (Pinus strobus) and/or Red pine (Pinus resinosa), two species native to Wisconsin that are suitable for transportation structure applications. They were visually graded No. 2 and better according to the Northeast Lumber Manufacturers Association (NELMA). Preservative pressure treatments included chromated copper arsenate (CCA) and Alkaline Copper Quaternary (ACQ). The configuration of the field test guardrail systems followed standard guardrail design criteria set by the Wisconsin Department of Transportation (Figure 1). The sawn lumber posts measured 6 x 8 in. with an overall post length between 72 and 78 inches. The minimum required embedment length is3ft 6 in., while the above ground length is approximately 28 inches. All posts evaluated were strong posts and were installed at 6-1/2 foot intervals along the roadway shoulder.

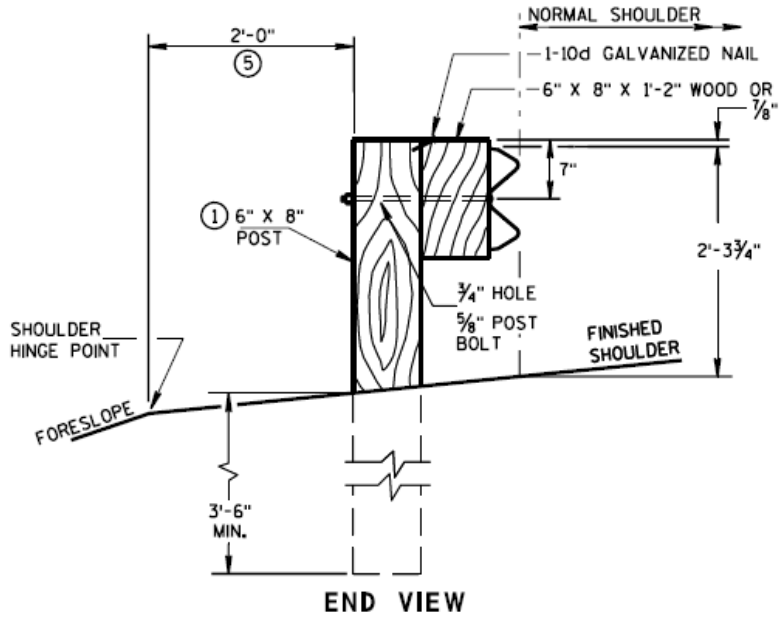

Figure 1 – Standard detail of timber post guardrail from WISDOT.

A total of 90 guardrail posts (40 old posts and 50 new posts) were evaluated at three different testing locations (Table 1). 20 older posts from both field test sites (40 total) were evaluated pre- removal (In-ground) and post-removal (out-of-ground). 20 new posts from both field test sites (40 total) were evaluated pre-installation (out-of-ground) and post-installation (in-ground). In addition, 10 new posts were evaluated at the FPL test site pre-installation (out-of-ground) and post-installation (in-ground).

Table 1 – Summary of guardrail post evaluations.

	Old posts		**New posts**	
Test site	**In ground**	**Out of ground**	**In ground**	**Out of ground**
FPL	--	--	10	10
Royalton	20	20	20	20
Merrimac	20	20	20	16[a]
Total	40		50	

[a]-three posts were lost and/or damaged during installation at the Merrimac test site;

Impact-Echo Acoustic Nondestructive Testing Approach

The nondestructive testing technique utilized to evaluate the guardrail posts is the "impact-echo acoustic method". The theoretical concept is based upon one-dimensional wave theory as it is applied to a homogeneous viscoelastic bar [7]. A mechanical impact at one end of the bar generates a compression stress wave that propagates through the material at a constant speed (C). Reflected waves are generated as the compression wave reaches the end of the bar. The wave continues to propagate through the bar until its energy is dissipated, or dampened. The compression wave speed (C) is related to the length of the bar and its time interval (Δt) as described in the following equation.

$$C =$$

The modulus of elasticity (MOE) is derived by using compression wave speed (C) and the mass density () of the bar, as follows:

$$MOE = C^2\rho$$

FPL Installed Guardrail Testing Site

A total of 10 new posts were evaluated pre-installation (out-of-ground) and post-installation (in-ground) at a testing site on the FPL campus (Figure 2). The Southern Pine posts measured approximately 6 by 6 by 78 inches and were treated with ACQ wood preservatives.

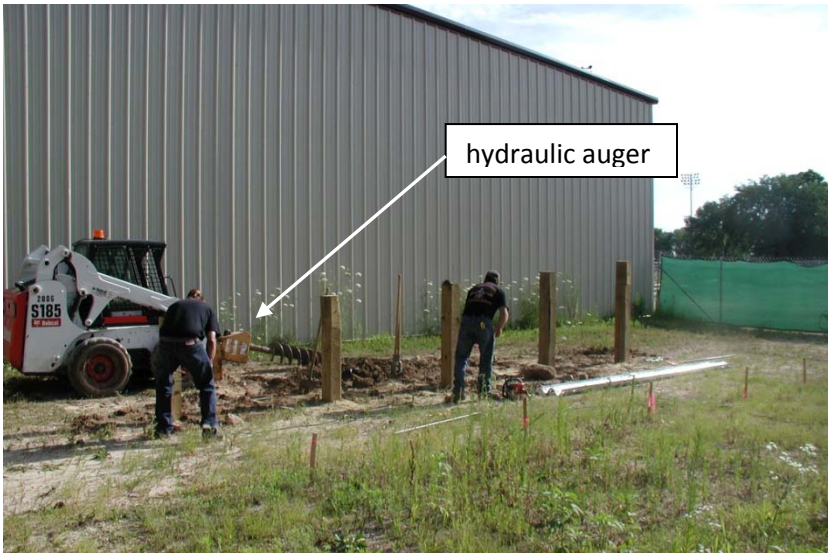

Figure 2 – Test guardrail posts being installed using pre-bored holes at FPL.

Guardrail posts were installed by a 3-person crew from Dane County Highway Department. Pre-boring the host holes and back filling was performed with hand tools. The soil type in the vicinity of the guardrail test sections is a silty loam.

Guardrail posts were installed in two parallel sections, each having treated timber posts at 75 inch intervals, and included timber offset blocks and steel w-beam rails, along the northern edge of the FPL campus. The embedded length of the post was intentionally varied (between 2.5 and 4.5 ft) in order to test the feasibility of nondestructive technique for estimating the post embedment length.

Testing trials involved the evaluation of several impact devices in order to determine impact conditions which produced the most consistent acoustic wave signals (Figure 3). Different sized

hammers and a spring-loaded (Pinger) device that was designed for more repeatable impact conditions were evaluated.

Figure 3 – Impact-echo NDE testing of in-service guardrail posts using various impact devices.

Guardrail Site Descriptions

Guardrail posts were evaluated at two field sites in the state of Wisconsin (Figure 4). Both sites contained old guardrail posts that served as approach railing at bridge crossing locations. At both bridge sites, posts are located in a roadway fill section with substantial slide slopes to facilitate drainage. The northernmost site is located in the city of Royalton in Waupaca County and is depicted in Figure 5. It is located along state highway 54 where it intersects the CN railroad line (GPS coordinates – N44º 24' 45.5", W88º 51' 28.7"). The posts were in service approximately 13 years based on WISDOT records review. According to the Natural Resource Conservation Service (NRCS) soil survey, the Royalton site contains a fine sandy loam, with 2 to 6 percent slopes. The southernmost site is located just west of the city of Merrimac in Sauk County and is depicted in Figure 6. It is located along state highway 113 approximately 1 mile west of Merrimac on the north side of the Wisconsin River (GPS coordinates –

N43º 22’ 22.9”, W89º 40’ 4.1”). Records were not available for the Merrimac site, but it is estimated that the posts were in-service for between 15 and 20 years. According to the NRCS Soil Survey, the Merrimac site contains a combination of soil types (Billett sandy loam with 12 to 20 percent slopes, eroded; and Plainfield loamy sand, 12 to 30 percent slopes). The general condition of the posts varied but several showed significant degradation at the end-grain exposed at the top surface (Figure 7).

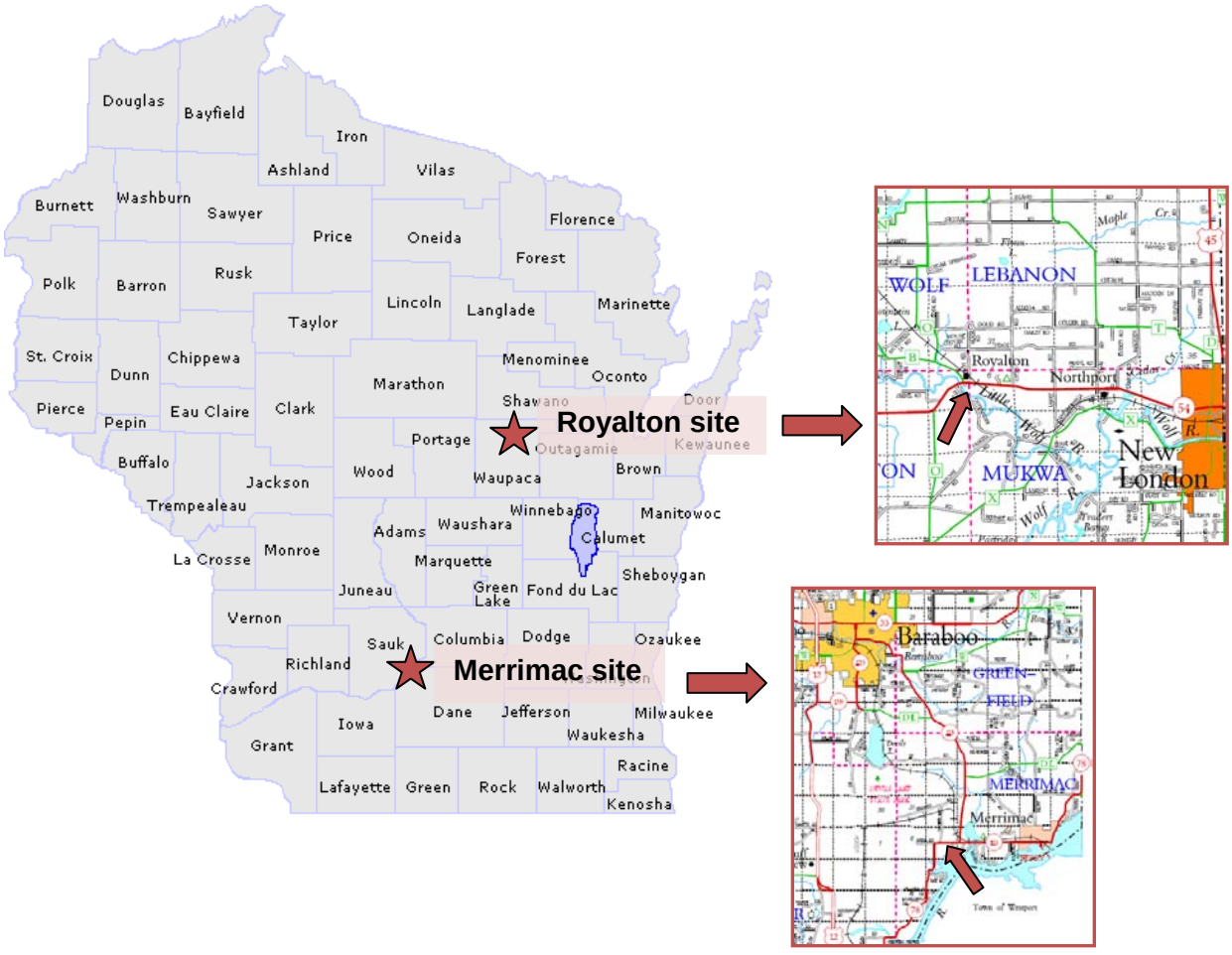

Figure 4 – Location map showing guardrail testing field sites.

Figure 5 – Field testing site near Royalton (Waupaca County) prior to removal of old guardrail posts.

Figure 6 – Field testing site near Merrimac (Sauk County) prior to removal of old guardrail posts.

Figure 7 – Condition of old guardrail posts after several years of service near Merrimac, Wisconsin.

Field Testing Procedures

A schematic of the general test setup is provided in Figure 8. Sound waves are introduced by an impact device at the exposed end grain surface on top of the timber post. A compression sound wave is transmitted along the longitudinal axis of the post and reflects upward after reaching the post bottom. An accelerometer connected at the top of the post near the impact zone captures the reflected wave response signal. The impact-echo acoustic response signals were recorded in the time domain using a National Instruments digital oscilloscope and a laptop computer. The acoustic signals were compiled as ASCI files and were subsequently evaluated in the frequency domain using spectral analysis.

Impact-echo acoustic response files were collected from all embedded guardrail posts (old & new) in a similar manner. The initial step was attaching the accelerometer to top of post using double-sided adhesive tape (In similar laboratory tests, the use of small lag screws at the post top end-grain to facilitate attachment of the accelerometer). Next was surface preparation of the post top surface for adequate impact conditions. The raised end-grain conditions which were typically encountered tended to severely reduce the imparted energy of the impact devices.

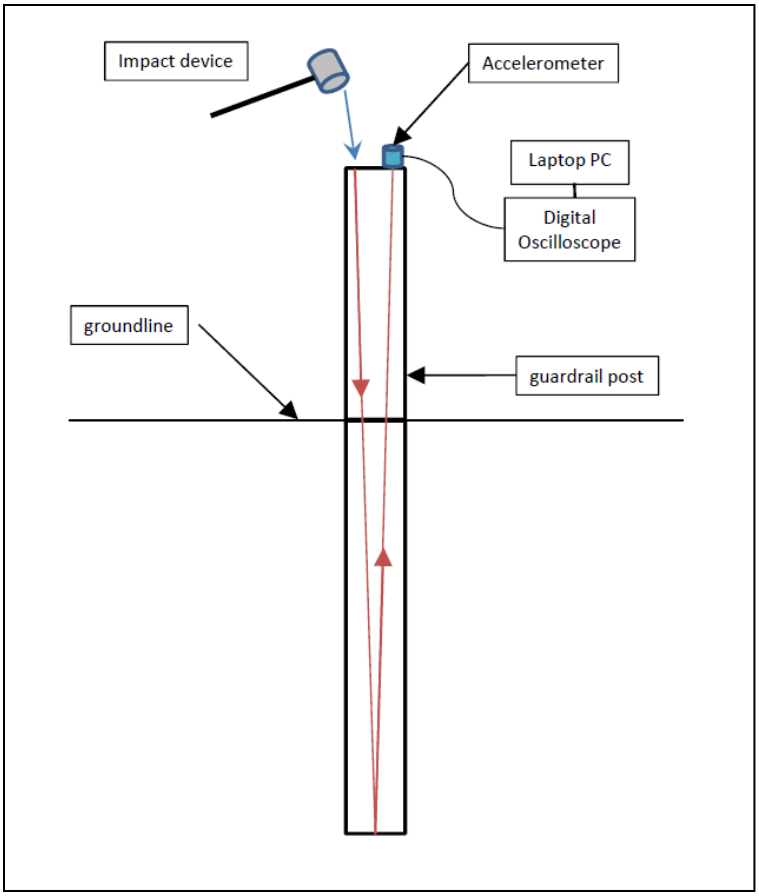

Figure 8 – Section view of impact-echo NDE evaluation technique used in the guardrail post inspections

A small hammer was typically used to flatten out the end grain conditions before testing was initiated. Impact-echo acoustic testing was conducted at each post using each of three different impact devices (Figure 3). Three test replicates were performed using each impact device and all response waveform signals were electronically stored in ASCI-formatted files for further analysis.

Frequency Spectrum Waveform Analysis

A customized graphical analysis routine was designed using Labview software package. Three methods were utilized in identifying the primary frequency of the guardrail posts. The first method involved evaluating the waveform in the time domain by selecting wave peaks, computing the frequency based upon the average interval, and computing a log-decrement curve. The second and third methods

involved Fast Fourier Transformation (FFT) techniques which converted the waveforms into the frequency domain. The second method included an FFT analysis of the entire waveform, while the third method included the selective interpretation of a subset of the waveform time spectrum in order to exclude complex data regions (Figure 9).

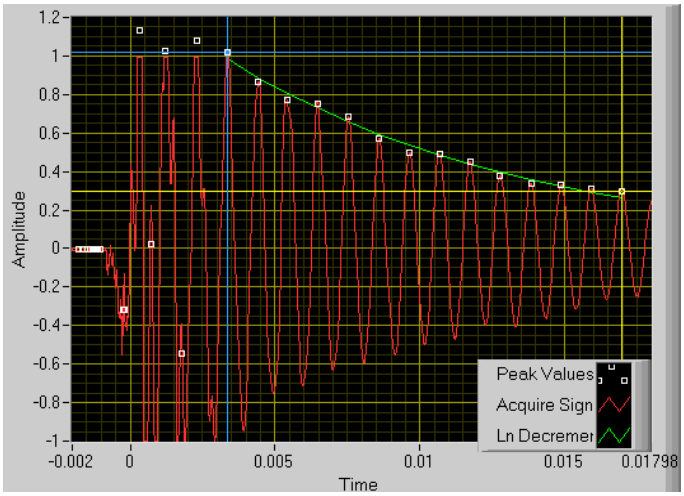

Figure 9 – Graphical analysis of impact-echo waveforms using a customized Labview software program.

The interpretation of the impact-echo waveforms included straightforward and challenging cases. In the straightforward case, the in-ground waveform contained a series of peaks and valleys at regular intervals with a relatively high damping ratio. In the more challenging case, the wave form contained peaks and valleys that were variable in magnitude and the intervals were inconsistent.

To aid interpretation, the response waveforms from the in-ground posts were comparatively analyzed to the out-of-ground test results performed in the laboratory. Figure 10 shows impact-echo acoustic response signals (time domain) and their associated Fast Fourier Transformation (FFT) signals (frequency domain) for Merrimac post M10. As can be observed, the in-ground response wave (between 6 and 14 milliseconds) and out-of-ground response wave (between 0 and 4 millisenconds) contains a portion of uniformly spaced peaks and valleys that gradually dissipate in towards zero energy. The in-ground response wave shows higher signal attenuation, possibly due to the soil contact boundary conditions. In addition, the dominant frequencies are easily interpreted from the frequency spectrum as

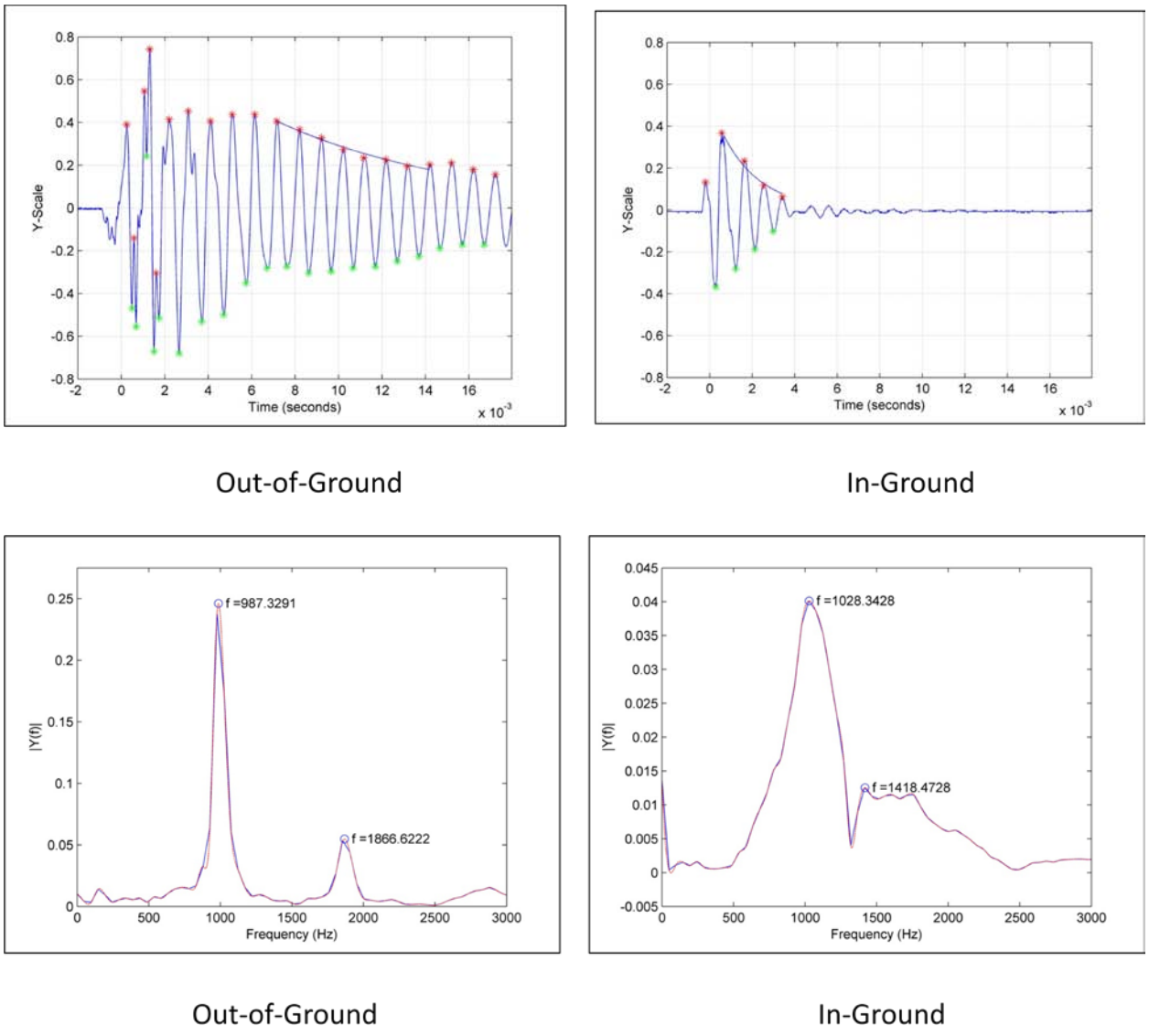

Figure 10 – Summary of impact-echo acoustic response signal (time domain) and their associated Fast Fourier Transformation (FFT) signals (frequency domain) for Merrimac post M10.

987 and 1,028 Hz. However, there is a slight upward shift in the dominant frequency present in the wave response signals for the in-ground guardrail posts.

Figure 11 shows a challenging case of data interpretation of the wave response for Merrimac guardrail post M13. The out-of-ground wave response (between 7 and 15 milliseconds) contains a portion of uniformly spaced peaks and valleys that gradually dissipate in towards zero energy. When analyzing the out-of-ground wave signal in the frequency domain, the dominant frequency is again easily

interpreted as 952 Hz. The in-ground response (time domain) analysis was more challenging as there was not any consistency present in the wave response peaks or valleys. When analyzed in the frequency domain, there are several peak frequencies present in the wave spectrum and it is not readily clear which value is dominant. In these challenging cases, we relied on the out-of ground frequency and selected an in-ground peak frequency that was slightly higher.

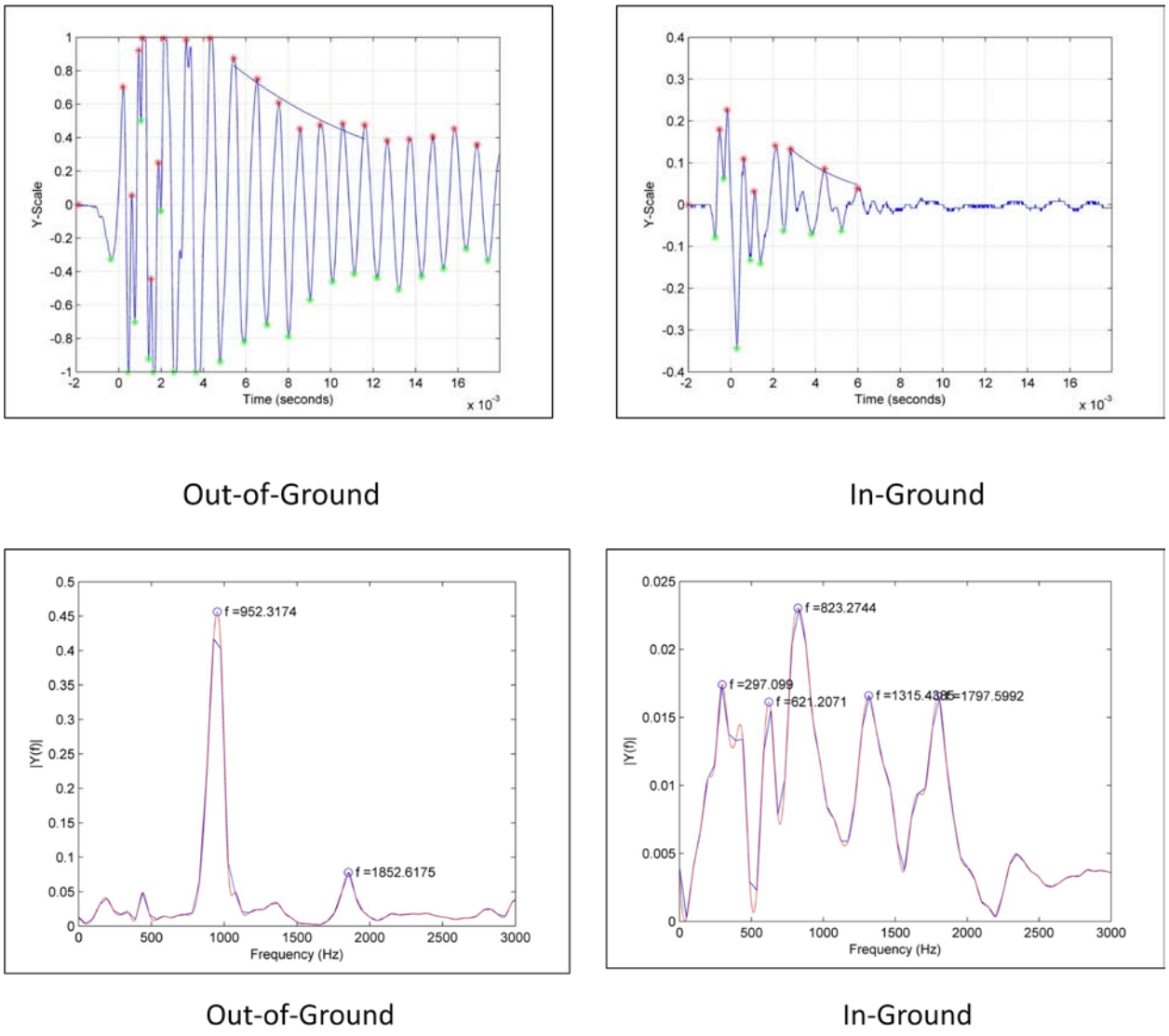

Figure 11 – Summary of impact-echo acoustic response signal (time domain) and the associated Fast Fourier Transformation (FFT) signals (frequency domain) for Merrimac post M13.

Laboratory Testing

All 20 guardrail posts were removed from each site shortly after field testing was completed and were transported to FPL for further testing (Figure 12). There was a substantial time lag (up to 7 months) between field and laboratory testing due to construction delays and laboratory scheduling conflicts. The laboratory testing included a physical examination of posts, a reevaluation with impact-echo acoustic techniques, and mechanical property testing.

Figure 12 – Removal of the guardrail posts for further evaluation in the laboratory.

Condition Assessment– The physical condition of all salvaged guardrail posts was assessed in the laboratory (Figure 13). However, due to construction and laboratory scheduling delays, there was a significant time lag between field and laboratory testing up to as many as 6 months. Measurements included dimensions, weights, photographs, defect diagrams, moisture content and specific gravity sampling, species identification, and transverse & longitudinal stress wave timing measurements. Moisture content and specific gravity measurements were collected in accordance with the requirements in ASTM D-4442 [6].

Figure 13 – Physical condition of each salvaged post was photographed and physical defects mapped.

Figure 14 – Impact-echo acoustic testing of salvaged guardrail posts in the laboratory.

Impact-Echo Acoustic Testing – These tests were repeated in a similar manner to the previously described field procedures, except that the posts were not embedded into the ground but positioned horizontally on test supports (Figure 14). In order to obtain effective coupling of the accelerometer onto the raised end-grain at the top of the post, a small lag screw was utilized in lieu of double-sided tape.

Stress wave measurements were collected using a Fakopp Microsecond Timer device. Longitudinal stress wave times were collected over the entire post length by attaching the spiked-transducers into the end grain. In order to gain a better understanding of the internal condition of the salvaged posts, a series of transverse stress wave measurements were performed at 6-inch intervals and along third-points (lines A and B) over the post width (Figure 15). Transverse stress wave times were collected by attaching the spiked-transducers at opposing locations in the wider (8-inch) post face (Figure 16).

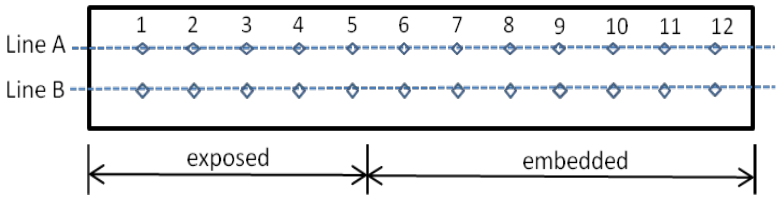

Figure 15 – Schematic of testing pattern used for transverse stress wave measurements.

Figure 16 – Transverse stress wave measurements on salvaged posts used to generate internal decay plots.

Mechanical Property Testing – The load response of all salvaged posts was evaluated under static loading conditions at the FPL's EMRSL laboratory. A cantilevered post testing setup (Figure 17) was used that approximated the guardrail field installation geometry. The bottom (embedded) portion of the post was fixed to a testing support block with three steel clamping plates (Figure 18). The center of the loading head was positioned 20.75 inches from the support edge and 7.875 inches from the post end to approximate the above-ground rail height.

Loading was applied at uniform rate of 0.33 inches per minute until failure was achieved when load-resistance dropped below 50 percent of the maximum load level. Applied loads were recorded with a 50-Kip calibrated load cell. Deflection measurements were taken with three LVDTs (Linear Variable Displacement Transformers) placed at the loading point, near the support edge, and at the fixed portion post end.

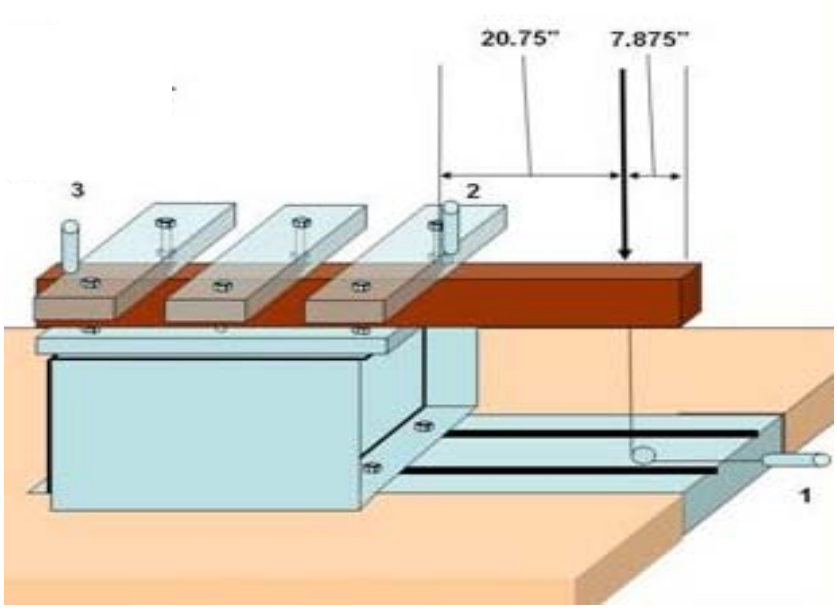

Figure 17 – Schematic of test setup used for cantilever bending stiffness and strength testing.

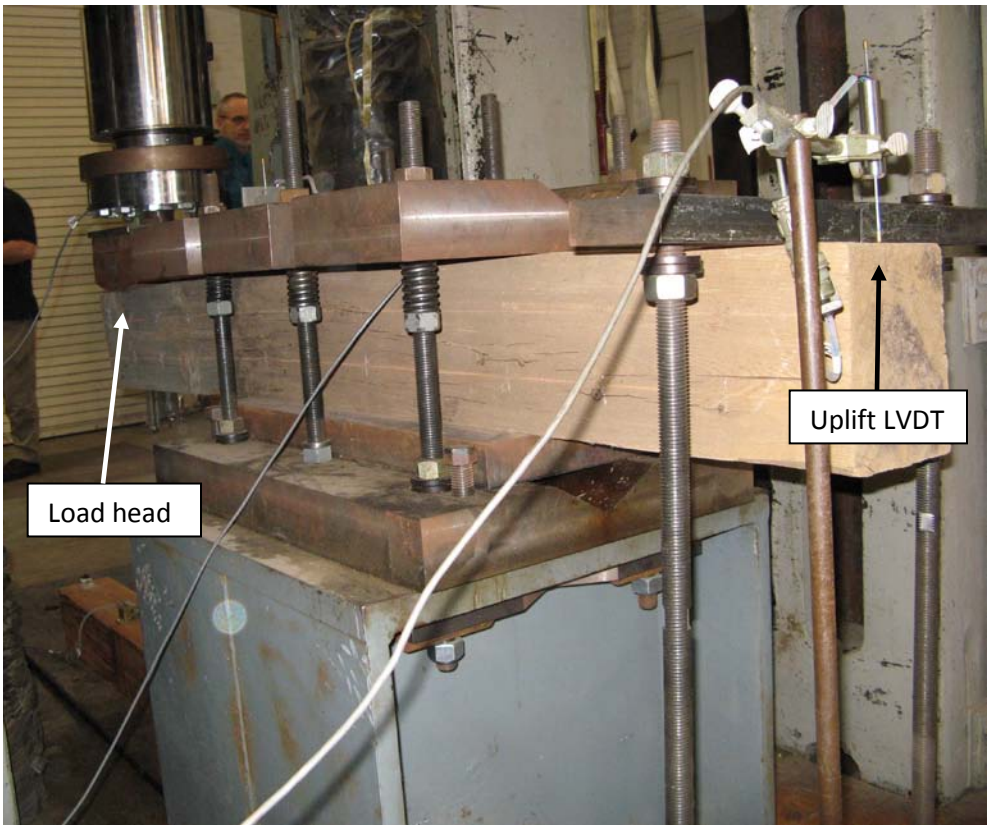

Figure 18 – Photograph of testing apparatus for cantilever bending stiffness and strength testing.

Maximum load, time-to failure, Modulus of Elasticity (MOE) and Modulus of Rupture (MOR) values were then determined. At the conclusion of testing, samples were removed from near the fracture zone for determination of moisture content and specific gravity values.

Field Testing – New Post Evaluations

Several tests were conducted on new guardrail posts around the time of installation at the field sites. First, impact-echo acoustic response signals were collected for out-of-ground test conditions (horizontally positioned on block supports, Figure 19) near the construction site. Post dimensions and weights were also collected to determine the density of the posts. Second, the posts were labeled with stainless steel identification tags before installation with a pneumatic machine (Figure 20). The new Merrimac site guardrail posts were installed in July 2009, while the Royalton site guardrail posts were

installed in November 2009. Photographs of the field testing sites, just after installation of the new guardrail posts, is shown in Figure 21. It should be noted that one post was destroyed and four other posts were lost during installation at the Merrimac site. In addition, three guardrail posts were unintentionally installed at a secondary location approximately 1.5 miles west of the original Merrimac field site along state highway 113 (GPS coordinates – N43º, 21', 48.8", W89º 41' 42.0"). Lastly, in-ground impact-echo testing was repeated in a similar manner as performed for the embedded old guardrail posts (Figure 22). Longitudinal "time of flight" stress wave measurements were collected in all posts in order to record its sound wave velocity which will be useful for condition assessments. This collective data set for the newly installed guardrail posts will provide a baseline reference for future acoustic-based inspections.

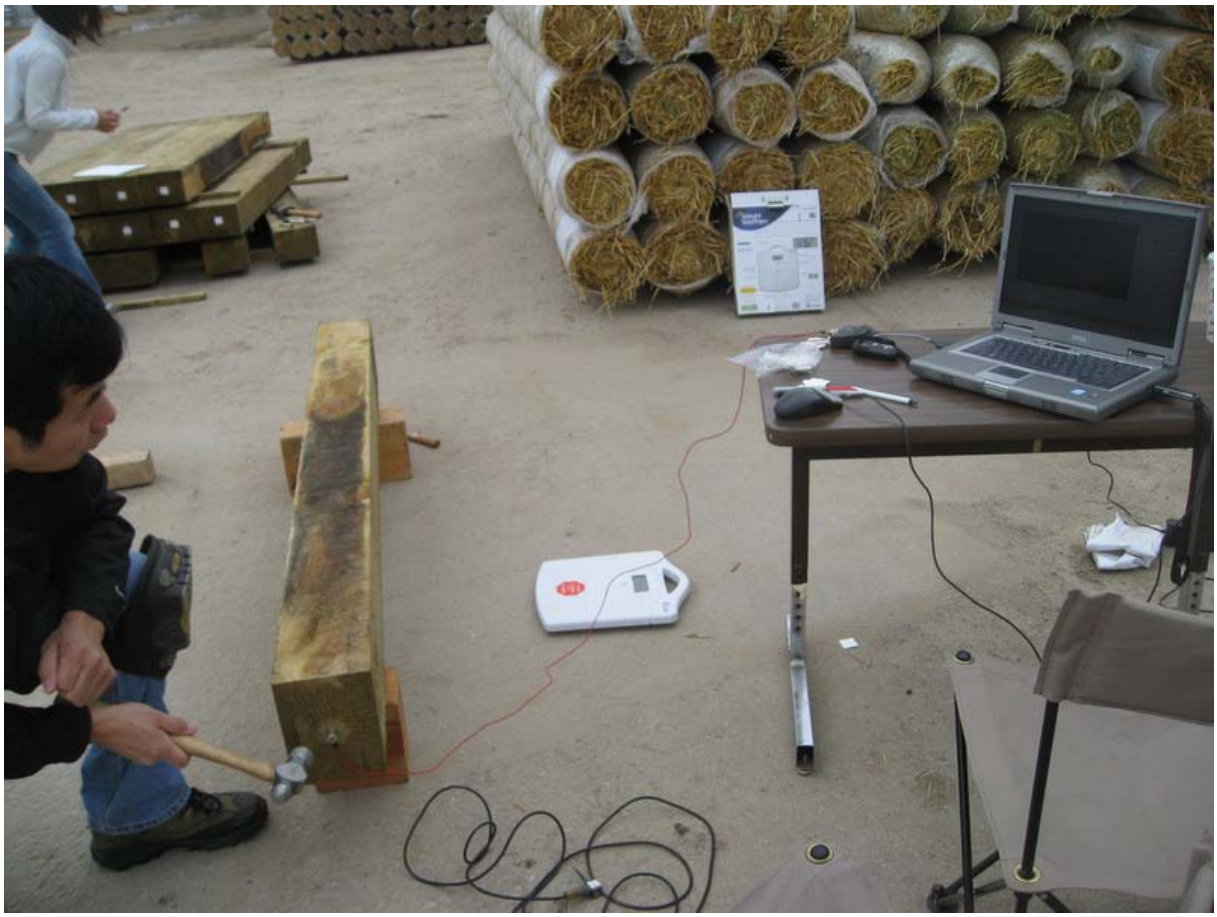

Figure 19 – Evaluating new posts prior to installation at the bridge site.

Figure 20 – Installation of new guardrail posts at the field test sites using a pneumatic machine.

Figure 21 – View of the new guardrail post installations at Royalton site (left) and Merrimac site (right).

Figure 22 – Impact-echo acoustic and stress wave testing of newly installed guardrail posts.

Results

Old Post Field Testing

Comparisons were made between FFT frequencies identified from the impact-echo acoustic response waveforms. Figure 23 compares the (In-ground vs. Out of ground) FFT frequencies observed from several impact devices utilized in field testing. The data tracks slightly below the "one-to-one" baseline of reference. The hammer and ping-device did not result in the most consistent results. The sledge hammer impact device resulted in the most consistent acoustic response waveforms for the older guardrail posts. The FPL testing on non-deteriorated new guardrail posts also identified the sledge hammer as the best impact device.

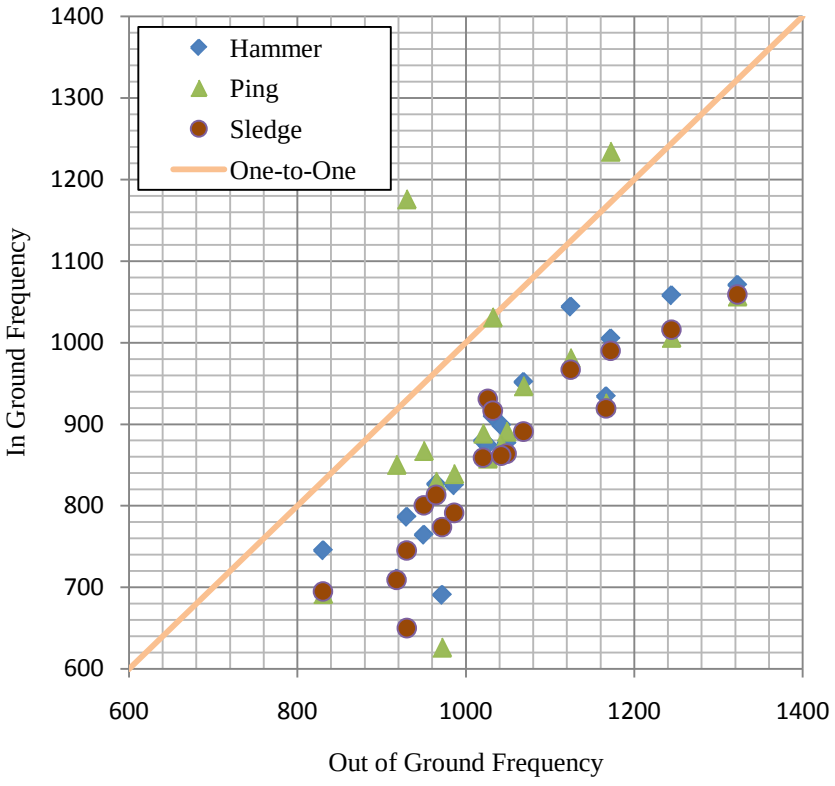

Figure 23 – Impact-echo acoustic NDE testing results using various impact devices at the Royalton site.

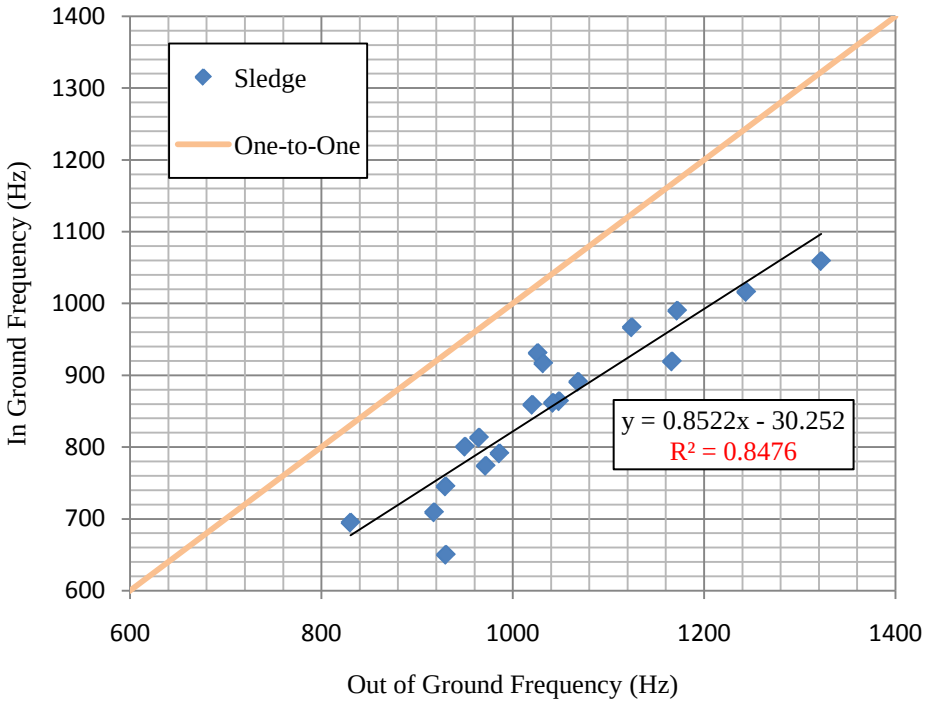

Figure 24 –Impact-echo results from the Royalton site with a sledge hammer impact device.

Figure 24 shows a strong correlation (r^2 = 0.8476) exists between in-ground and out-of-ground FFT frequencies for the Royalton guardrail posts. This strong relationship demonstrates that the impact-echo acoustic technique is a feasible inspection approach for timber guardrail posts. However, the correlation between in-ground and out-of-ground FFT frequencies for the Merrimac site was weaker with an r^2 = 0.5861 (Figure 25). The Merrimac posts were assumed to be older than the Royalton posts (13 years in-service) and had substantially higher moisture contents levels. The Merrimac posts have an average moisture content of 88 percent with a standard deviation of 38.4 ranging from 28 through177 percent. While the Royalton posts had an average moisture content of 27.7 percent with a standard deviation of 7.0 ranging from 14.5 through 37.9 percent. It was not clear what caused this dramatic moisture content contrast between the guardrail post test sites, but the super-saturated Merrimac posts

definitely affected the impact-echo acoustic testing results. A moisture content data summary is provided in Table 2.

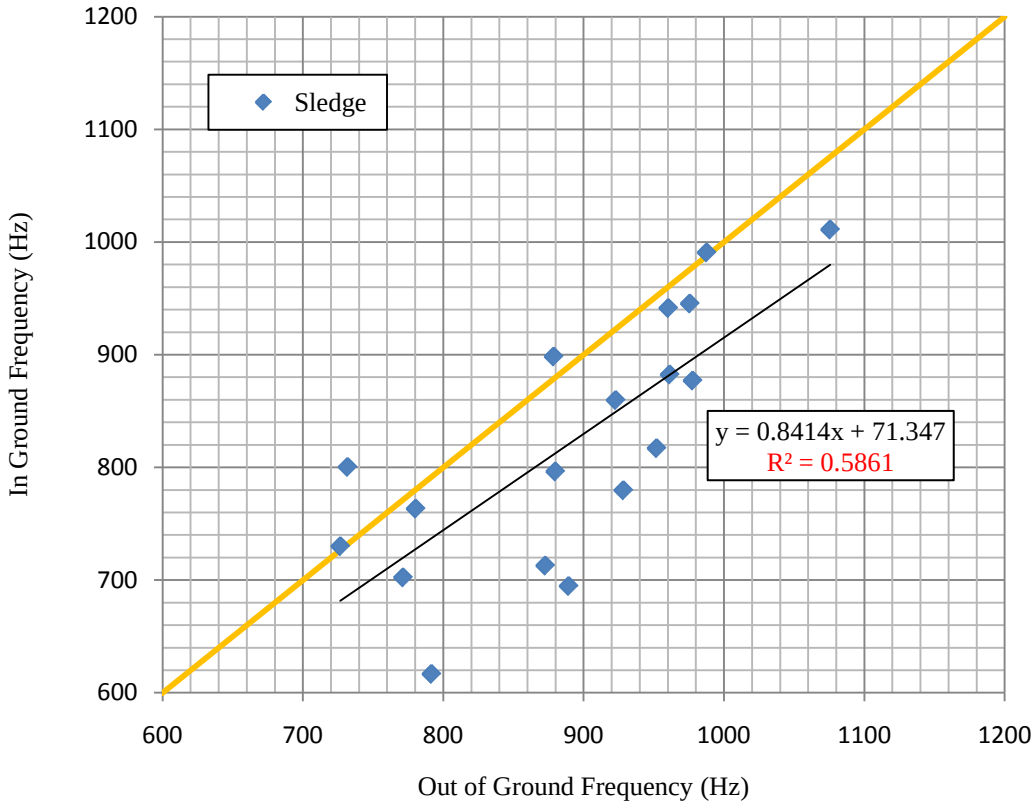

Figure 25 – Merrimac field testing results using sledge hammer impact device.

Laboratory Testing of Old Posts

A cantilevered-bending failure for Royalton post specimen number 19 is shown in Figure 26. The failure zone typically occurred near the ground line of the post. In this case, however, the presence of a large edge-knot caused the post to fail prematurely. More stringent visual grading of the posts near the ground line zone could help to achieve more consistent residual post strengths. Figure 27 shows a typical load-displacement curve from Merrimac post specimen number 13. This post failed at a load higher than 12 Kips and with more 0.60 inches of deflection at the cantilevered end. The MOR values are summarized in the following figures: Merrimac posts (Figure 28) and Royalton posts (Figure 29). The

Merrimac posts had an average MOR of 3,161 lb/in.^{2} with a standard deviation of 762 over a range extending from 1,510 through 4,031 lb/in.^{2} The Royalton posts had an average MOR of 2,712 lb/in.^{2} with a standard deviation of 980 over a range extending from 1,072 through 4,261 lb/in.^{2}.

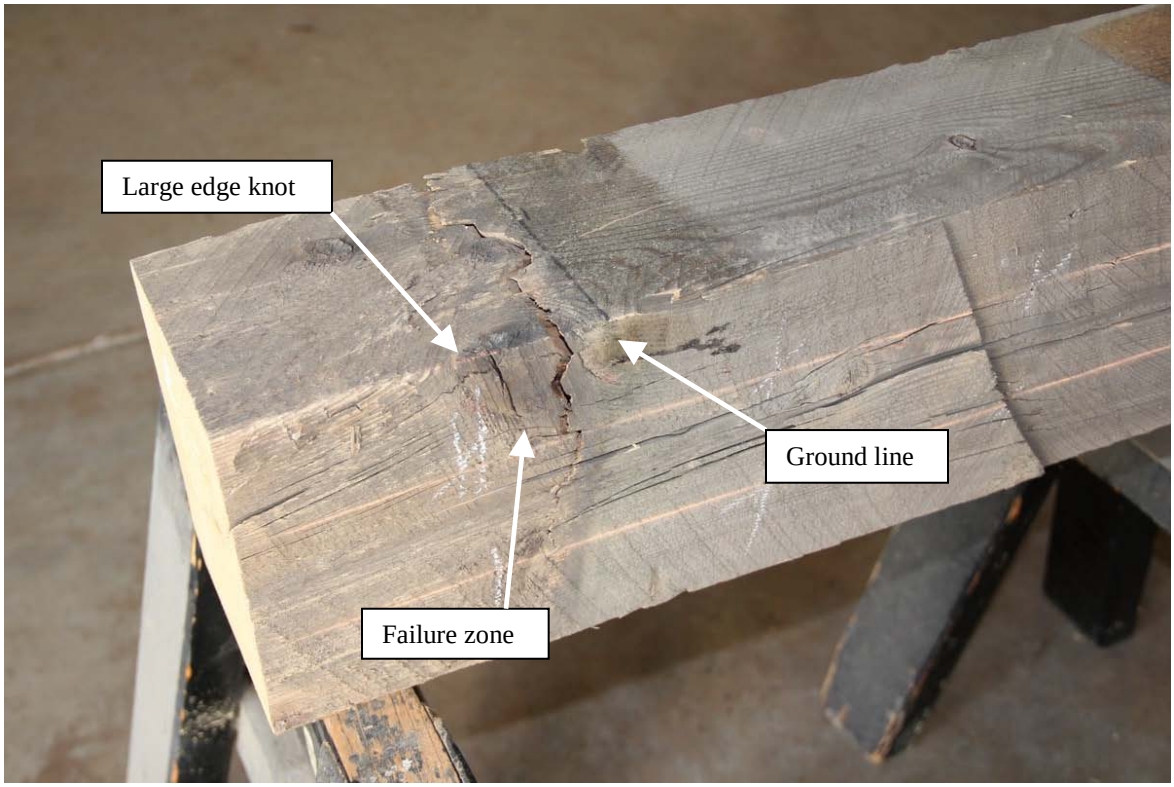

Figure 26 – Failed cantilever bending specimen R19 from the Royalton test site. Note the edge knots at the failure zone near the ground line.

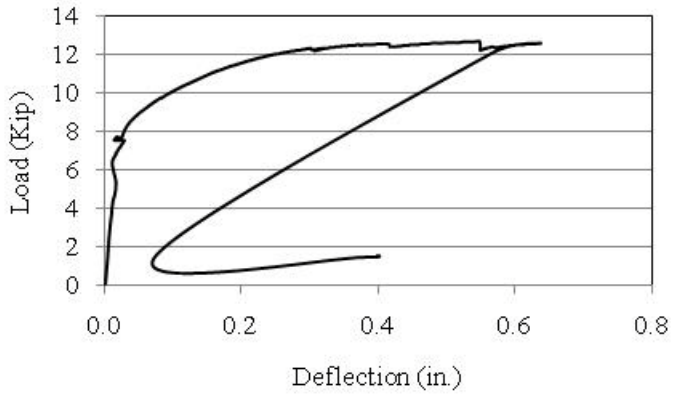

Figure 27 – Load-deflection curve from cantilevered bending test of Merrimac Post M13.

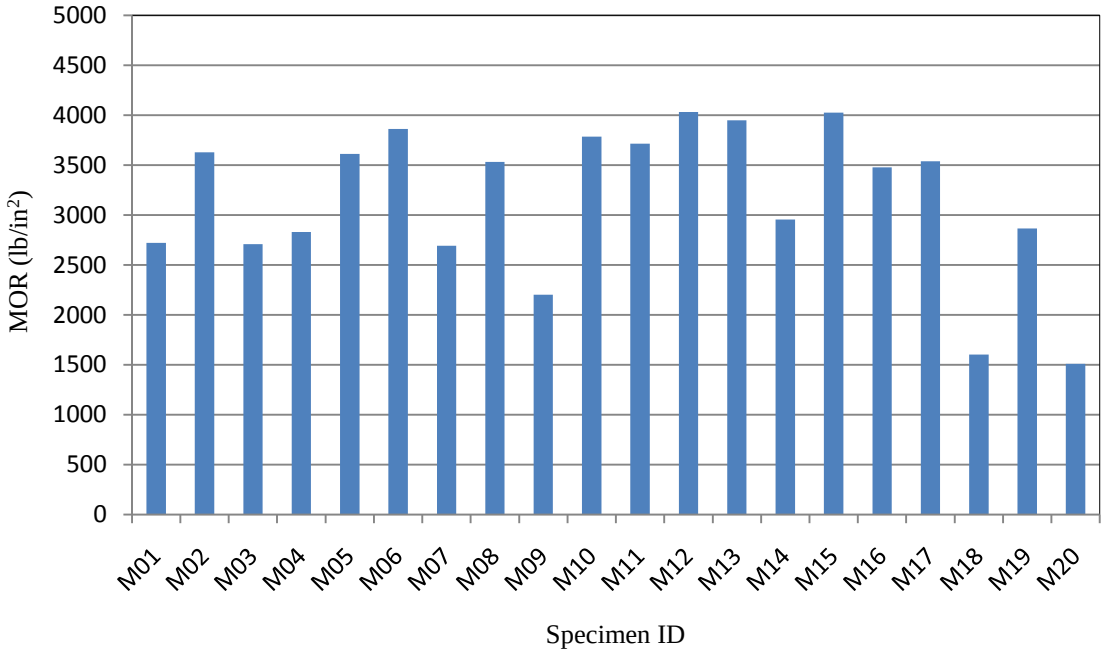

Figure 28 – Cantilever bending strength of the salvaged Merrimac guardrail posts.

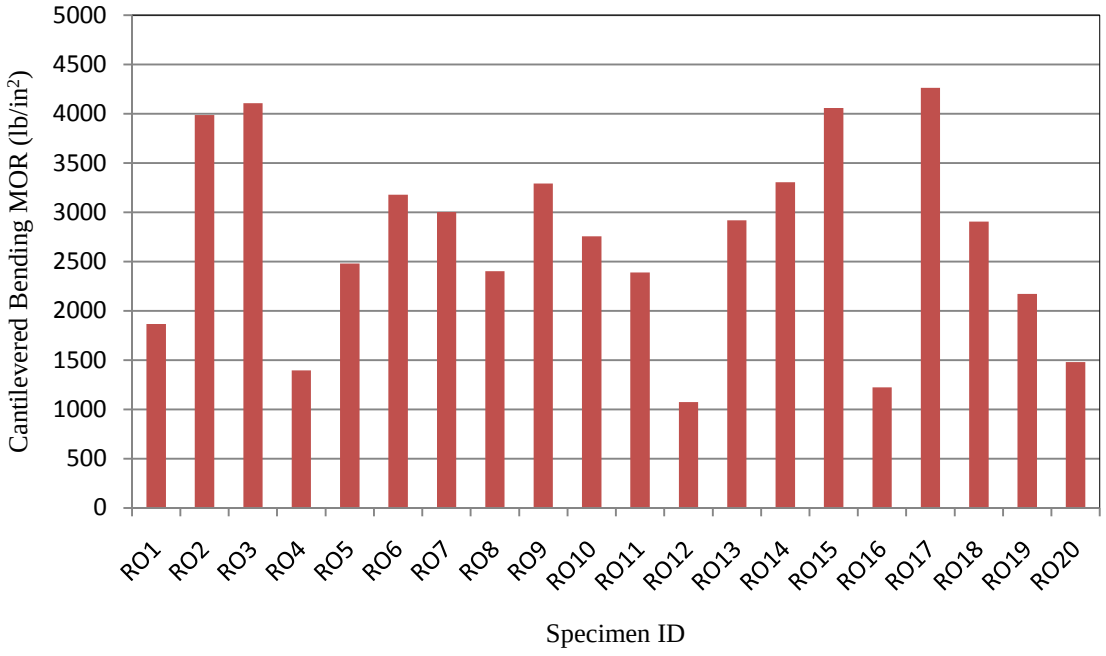

Figure 29 – Cantilever bending strength of the salvaged Royalton guardrail posts.

Table 2 – Summary of (old post) guardrail data.

Specimen ID	FFT Frequency (Hz) In-ground*	FFT Frequency (Hz) Out-of-ground	MC (%)	Specific Gravity	MOE^{SW} ($lb/in.^2$)	MOR ($lb/in.^2$)
Royalton Site						
R01	709	918	38	0.29	0.86	1866
R02	891	1068	27	0.33	1.09	3984
R03	1059	1322	21	0.35	1.57	4105
R04	801	950	35	0.29	0.77	1396
R05	864	1048	33	0.34	1.09	2477
R06	859	1020	28	0.30	0.88	3177
R07	813	965	26	0.33	1.05	3001
R08	774	972	35	0.31	0.85	2402
R09	1016	1244	30	0.40	1.73	3289
R10	791	986	15	0.35	0.90	2755
R11	931	1026	33	0.39	1.08	2388
R12	--	--	24	0.25	0.80	1072
R13	650	930	20	0.34	0.78	2916
R14	990	1172	16	0.33	1.10	3303
R15	917	1032	33	0.45	1.23	4058
R16	745	930	29	0.30	0.81	1222
R17	919	1166	16	0.32	1.07	4261
R18	862	1042	31	0.33	1.01	2906
R19	967	1124	32	0.35	1.17	2172
R20	695	830	31	0.39	0.67	1480
Merrimac Site						
M01	945	976	62	0.37	1.11	2720
M02	898	879	63	0.44	1.12	3627
M03	695	889	95	0.32	1.00	2709
M04	941	960	94	0.30	1.12	2828
M05	702	771	69	0.42	0.82	3610
M06	713	873	82	0.33	1.95	3861
M07	800	732	55	0.34	0.93	2693
M08	--	--	58	0.30	0.94	3530
M09	--	--	129	0.33	1.13	2202
M10	991	988	131	0.33	1.41	3784
M11	877	978	72	0.39	1.29	3715
M12	796	880	82	0.34	0.90	4031
M13	817	952	107	0.35	1.17	3948
M14	860	923	82	0.34	1.09	2953
M15	882	961	28	0.32	1.03	4024
M16	1011	1076	37	0.33	1.28	3477
M17	780	928	165	0.31	1.18	3536
M18	617	792	84	0.31	0.72	1602
M19	730	727	84	0.37	0.95	2866
M20	763	780	177	0.29	0.92	1510

*-data from sledge hammer as impact device; double dash denotes no data available;

The relationship between MOE and MOR for both sets of guardrail posts is provided in Figure 30. In this case, the MOE was derived from the longitudinal stress-wave data which has been proven to be a reliable method for estimating member stiffness. The correlation for the Merrimac posts was relatively low with an $r^2 = 0.1944$. A stronger correlation was found for the Royalton posts with an $r^2 = 0.3907$. This marked difference is most likely attributed to the vast difference in in-situ moisture contents of the posts.

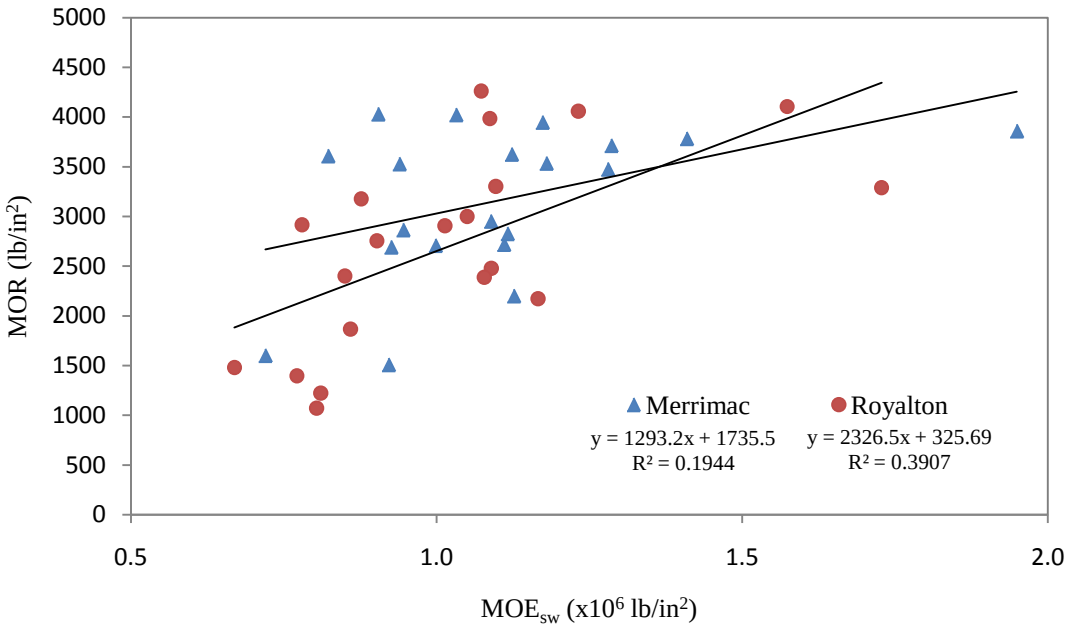

Figure 30 – Comparison of MOR vs. MOE for both sets of salvaged guardrail posts.

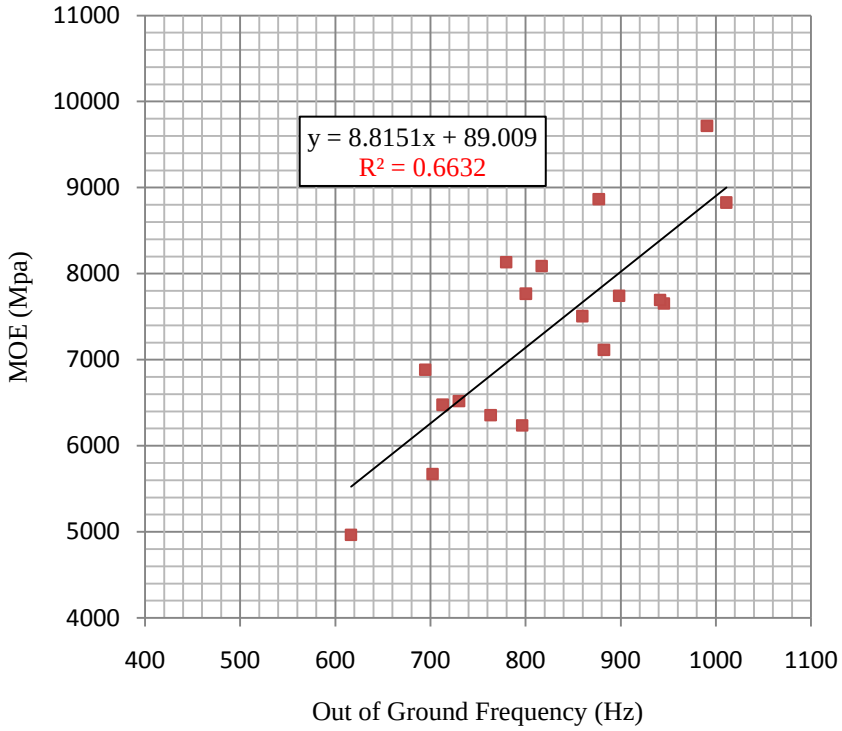

Figure 31 – Comparison of out-of-ground FFT frequency versus the Modulus of Elasticity (MOE) of the salvaged Merrimac guardrail posts.

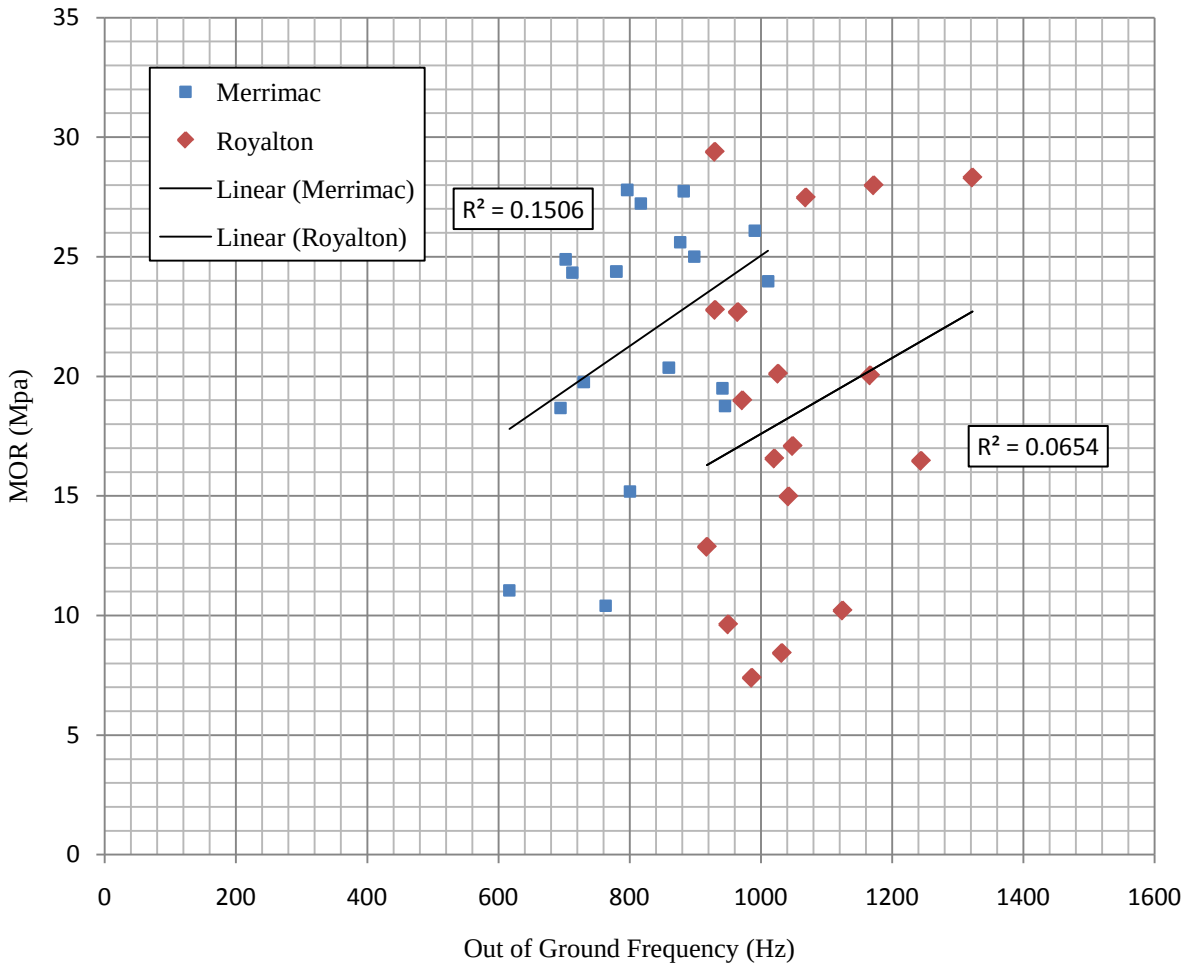

Figure 32 – Comparison of out-of-ground FFT frequency versus the Modulus of Rupture (MOR) of the salvaged guardrail posts.

FFT Frequency and Bending Property Comparison

Figure 31 compares the out-of-ground FFT post frequency with the MOE values for the Merrimac posts. As expected, there is a strong relationship with an r^2 value of 0.6632. As previously noted, longitudinal stress wave velocity has a strong correlation with the member stiffness and density. Figure 32 compares the out-of-ground FFT frequency and the MOR values for both post sets. These relationships are not very strong (Merrimac r^2 = 0.1506; Royalton r^2 = 0.0654) and is attributed to a number of factors. First, the level and presence of decay activity within the guardrail post section can dramatically affect the residual strength if located in the high stressed zone near ground line. This was the case for many posts. Second,

the occurrence of natural defects (deep checks and knots) near the high stressed zone can also lead to low strength values. Third, the much higher moisture contents found in the Merrimac posts will result in lowering their MOR values.

Field Testing – New Posts

A summary of the field data collected from the new guardrail posts both pre- and post-installation is provided in Table 3. Included are several data sets collected on the mixed red/white pine posts. FFT frequency values from impact-echo acoustic NDE testing performed both pre-installation (out-of-ground) and post-installation (in-ground). Weights and dimensions were collected and density values were derived. Lastly, stress wave values were collected in order to estimate the specific wave velocity for each post. This collective data set should be helpful; creating a baseline of reference as future guardrail post inspection work is undertaken.

Table 3 – Summary of (new post) guardrail data.

Specimen ID tag	FFT Isolated Frequency (Hz) Out-of-ground	In-ground[a]	Weight (lbs)	Density[b] (pcf)	Stress Wave Rate[c] (µs/ft) Side 1	Side 2
Royalton Site						
CB424	986	919	77.4	35.7	61	68
CB425	977	1448	92.8	42.8	68	69
CB426	852	970	78.8	36.4	80	81
CB427	1031	982	79.0	36.5	73	64
CB428	990	1227	66.2	30.6	76	73
CB429	864	1283	81.4	37.6	75	103
CB430	1049	957	68.0	31.4	68	65
CB431	820	1139	76.6	35.4	106	74
CB432	1002	1126	77.2	35.6	66	70
CB433	910	1374	71.4	33.0	68	73
CB434	969	994	78.2	36.1	73	75
CB435	846	1251	71.2	32.9	81	93
CB436	914	1057	67.2	31.0	76	71
CB437	992	1344	68.4	31.6	64	73
CB438	936	909	96.0	44.3	78	77
CB439	1000	1173	66.2	30.6	68	73
CB440	881	928	95.0	43.8	95	91
CB441	1021	1135	79.2	36.6	80	68
CB442	873	968	77.4	35.7	70	82
CB443	1018	1050	62.2	28.7	64	78
Merrimac Site						
E51	690	897	71.4	33.0	87	92
E52	584	--	78.2	36.1	--	--
E53	745	--	73.6	34.0	--	--
E54	883	824	75.2	34.7	92	72
E55	740	667	68.2	31.5	77	103
E56	688	--	71.2	32.9	92	100
E57	775	679	74.4	34.3	90	98
E58	779	--	84.6	39.0	82	73
E59	788	689	78.6	36.3	77	91
E60	876	785	73.0	33.7	68	79
E61	792	538	72.4	33.4	79	92
E62	773	584	81.2	37.5	79	78
E63	784	552	67.2	31.0	--	--
E65	760	685	67.2	31.0	70	80
E66	744	839	63.0	29.1	83	76
E67	731	--	70.8	32.7	--	--
E67	783	765	69.2	31.9	80	75
E68	846	583	68.0	31.4	72	71
E69	886	637	65.6	30.3	--	--
E70	735	764	74.0	34.2	99	83

a-based on measured post dimension and weight; b-double dash denotes a guardrail post not found after installation; c-measured at above-ground portion of the post over a 2 foot travel distance;

Summary & Conclusions

The main motivation for this work was the development of a nondestructive field inspection protocol for guardrail posts to support asset management practices. This study evaluated the effectiveness of impact-echo acoustic NDE testing techniques for the inspection of in-service timber guardrail posts. Several posts were evaluated while in-the-ground at two field sites in southern and central Wisconsin. In addition, the same set of guardrail posts were salvaged for further laboratory study, including cantilevered-bending ultimate strength tests.

The following conclusions are provided based on the field and laboratory testing conducted on old guardrail posts.

- Impact-echo acoustic testing is a viable NDE technique for the inspection of timber guardrail posts in-service. However, it is not yet a practical tool for field inspection purposes. Further additional work is needed to develop a fully-automated and practical inspection tool.

- The FFT wave frequencies were compared between the In-ground and Out-of-ground for the posts removed after several years of service. The Royalton posts had a fairly strong relationship ($r^2 = 0.8476$) which proved the concept is suitable for guardrail post inspections. The Merrimac post relationship was not as strong ($r^2 = 0.5861$) likely due to much higher in-situ moisture content levels.

- FFT frequencies occurred within the range of 700 to 1200 Hz. In-ground FFT frequencies were lower than their out-of-ground FFT frequency counterpart. The soil-post interface boundary conditions resulted in distorted wave responses and relatively higher attenuation rate. This presented additional challenges for FFT wave analysis in the frequency spectrum.

- Visual assessments of the guardrail post exterior condition revealed major defects (splits, knots greater than 1-inch diameter, and large splits) in the critical stress zone (within +/- 12 in. of the

ground line). Only 3 of 20 total Merrimac posts and 2 of 20 Royalton posts did not have major defects in the critical stress zone. More stringent grading procedures could reduce the allowable defect size in this critical zone which would result in higher average cantilever-bending strength MOR values.

- Oven-dry moisture contents recorded shortly after cantilevered-post bending tests, revealed vastly different results for the guardrail post sets. The Merrimac posts have an average moisture content of 88 percent with a standard deviation of 38.4 ranging from 28 through177 percent. While the Royalton posts had an average moisture content of 27.7 percent with a standard deviation of 7.0 ranging from 14.5 through 37.9 percent. It was not clear as to the cause of the dramatic difference in in-situ moisture content, but it certainly had an effect on the impact-echo acoustic wave testing results. The speed of sound waves is directly affected by moisture content levels.

- Static cantilever-post bending in the elastic range indicated average MOE values of 1.03 X 10^6 lb/in.^{2} for the Royalton posts and 1.10 X 10^6 lb/in.^{2} for the Merrimac posts. The post bending stiffness data for the Merrimac posts had good correlation (r^2 = 0.6632) with the out-of ground FFT frequency data.

- Cantilevered post bending strength testing indicated average MOR values of 2,712 lb/in.^{2} for the Royalton posts and 3,161 lb/in.^{2} for the Merrimac posts. This residual strength data for the salvaged guardrail posts had a weak correlation with respect to the out-of-ground FFT frequency data (r^2 = 0.1506 for Merrimac and r^2 = 0.0654 for Royalton posts).

- Stress wave (transverse orientation) scanning of the salvaged guardrail posts revealed areas of internal decay. Most of the internal decay was detected within the mud line (+/- 1 ft about the ground line). For individual contour plots of each salvaged post, see the Appendix.

Recommendations

The following recommendations are suggested to guide future work regarding timber guardrail post inspection and monitoring.

- Monitor the condition of the new guardrail posts at each field site for their entire service life. Impact-echo acoustic testing data should be collected at 3-year intervals, in addition to periodic visual assessments.
- Additional development work is needed to achieve a user-friendly inspection tool based on impact-echo acoustic techniques. Work should focus on new automated signal processing algorithms and housed in a hand-held computer device as this may provide the best solution for field inspectors.
- Conduct impact-echo testing for a companion set of guardrail posts at an additional northern Wisconsin field site. These results can be comparatively analyzed with the southern and central sites to characterize any climatic effects on guardrail longevity.
- Evaluate the effectiveness of a resistance micro-drilling tool in assessing the internal condition of guardrail posts. This minimally-invasive NDE technique provides a relative-density profile of the post's internal integrity using a very small diameter drilling bit. It is commonly used to determine the degree of sound wood remaining at critical locations. Data collection should be focused near the ground line of the post with 45º downward drilling orientation. This technique may be a reliable indicator of post condition and residual strength and should be further investigated

References Cited

[1] Kennedy J.C., Plaxico C.A., and Miele C.R.; Transportation Research Record: Journal of the Transportation Research Board, No. 1984, Transportation Research Board of the National Academies, Washington, D.C. pp. 69–81. 2006.

[2] Chen S., Kim R.; Condition Assessment of Installed Timber Piles by Dispersive Wave Propagation. Transportation Research Record: Journal of the Transportation Research Board, No. 1546, Transportation Research Board of the National Academies, Washington, D.C. pp. 112-120. 1996.

[3] Holt J.D., Chen S., and Douglas R.A. Determining lengths of installed timber piles by dispersive wave propagation. Transportation Research Board, National Research Council, Transportation Research Record No. 1447, pp. 110-115. 1994.

[4] ASTM. Standard D5882. Standard test method for low strain impact integrity testing of deep foundations. Conshohocken, PA: American Society for Testing and Materials. 2007.

[5] White D., Mekkawy M., Klaiber W., and Wipf T.; Investigation of Steel-Stringer Bridges: Substructure and Superstructure, Volume II. Center for Transportation Research, Iowa State University. 2007.

[6] ASTM. D4442 - Direct moisture content measurement of wood and wood-based materials. West Coshocton, PA. 2007.

[7] Ross, R.J. Nodestructive Evaluation of Wood. Madison, WI: Forest Products Society. 210 p. 2002.

This page left blank intentionally.

Appendix

Stress Wave Scanning Results

The legend key below applies to all the color-coded internal condition plots:

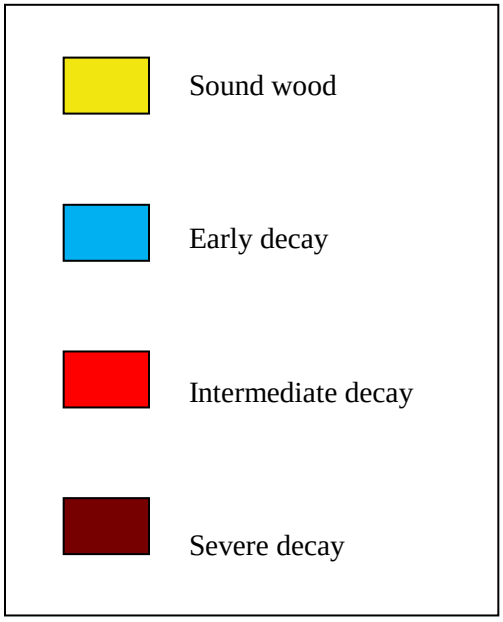

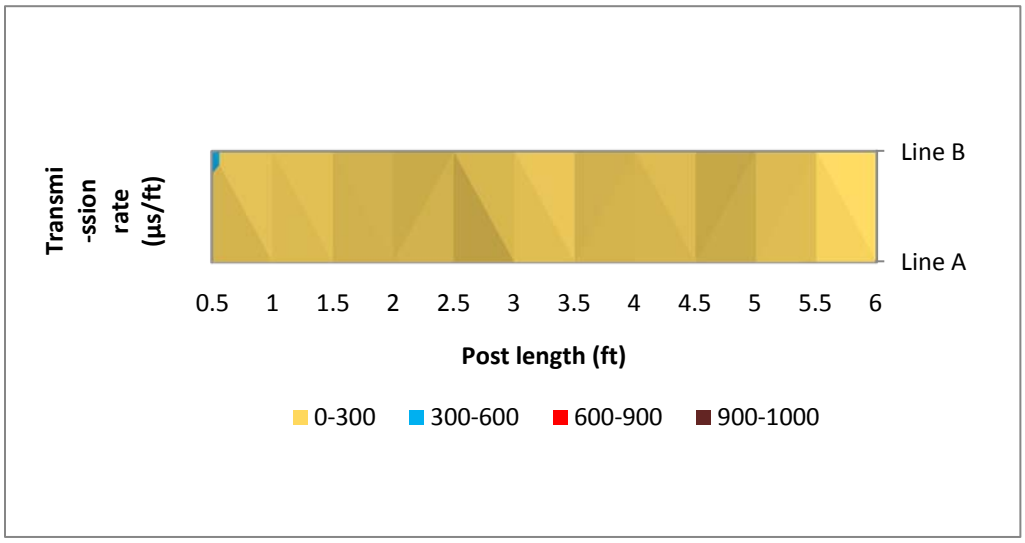

Figure A1. Results from perpendicular-to-grain stress wave scanning for R01 at Royalton site

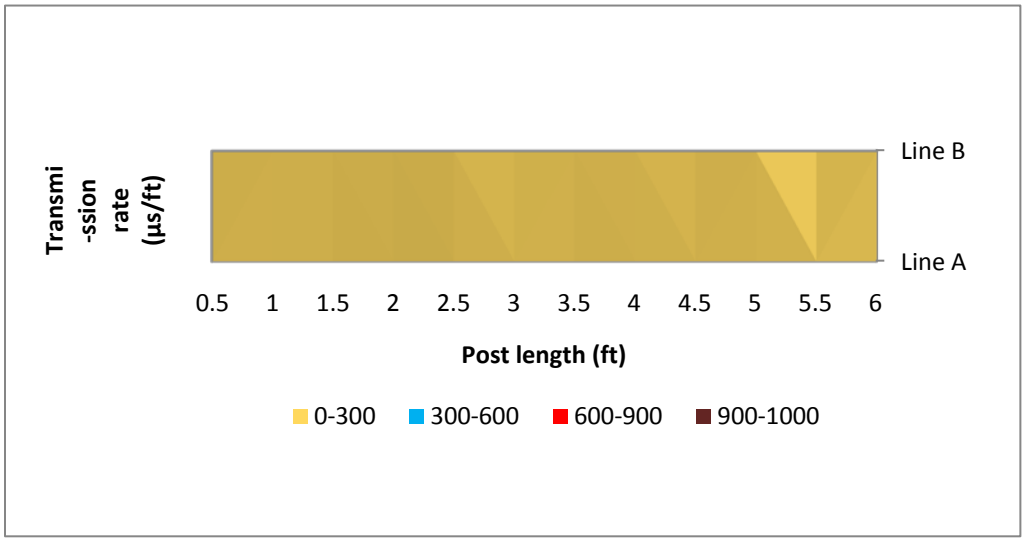

Figure A2. Results from perpendicular-to-grain stress wave scanning for R02 at Royalton site

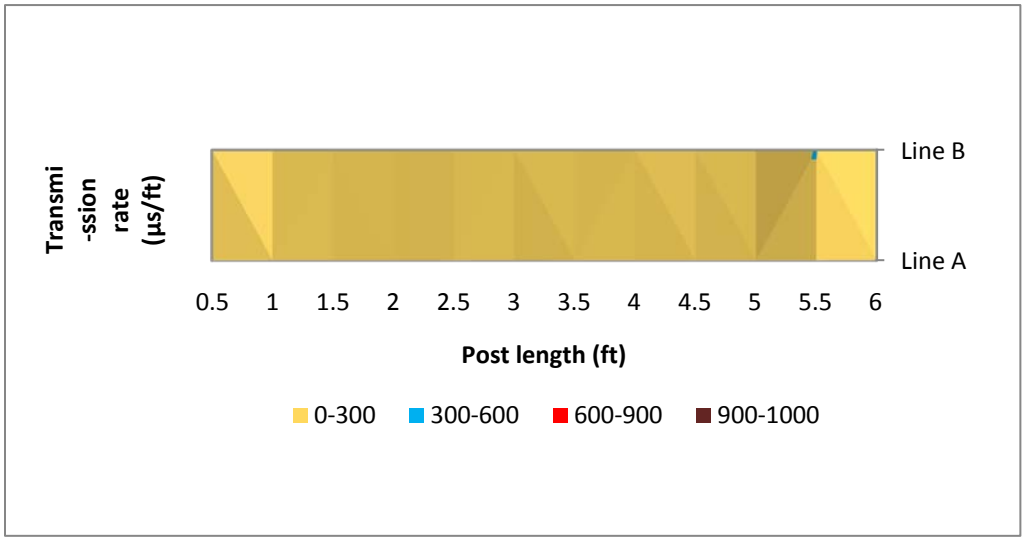

Figure A3. Results from perpendicular-to-grain stress wave scanning for R03 at Royalton site

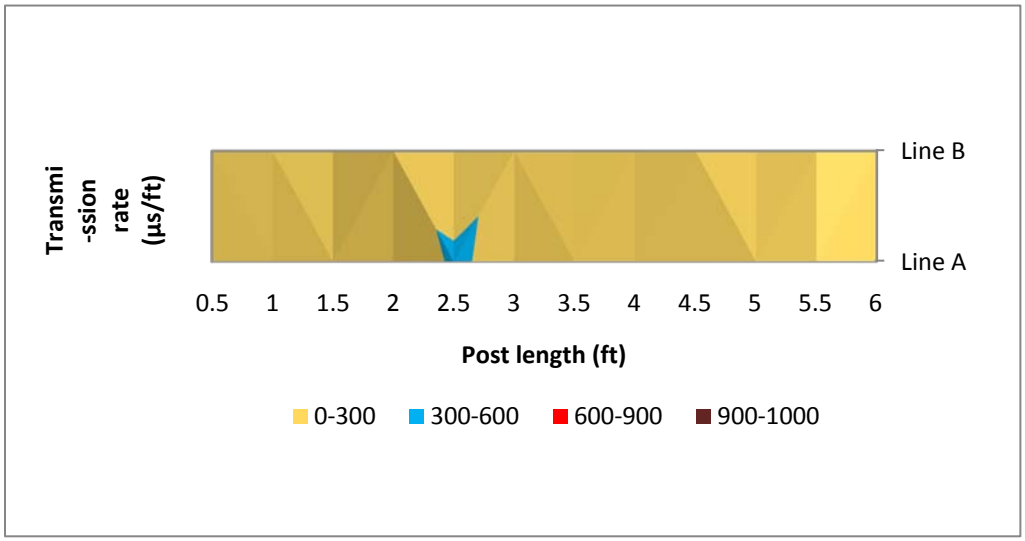

Figure A4. Results from perpendicular-to-grain stress wave scanning for R04 at Royalton site

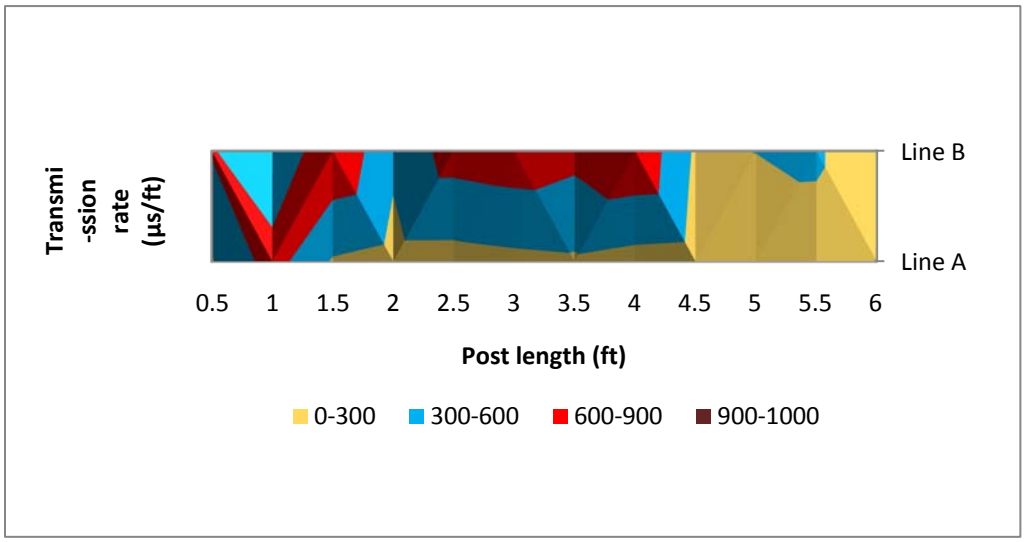

Figure A5. Results from perpendicular-to-grain stress wave scanning for R05 at Royalton site

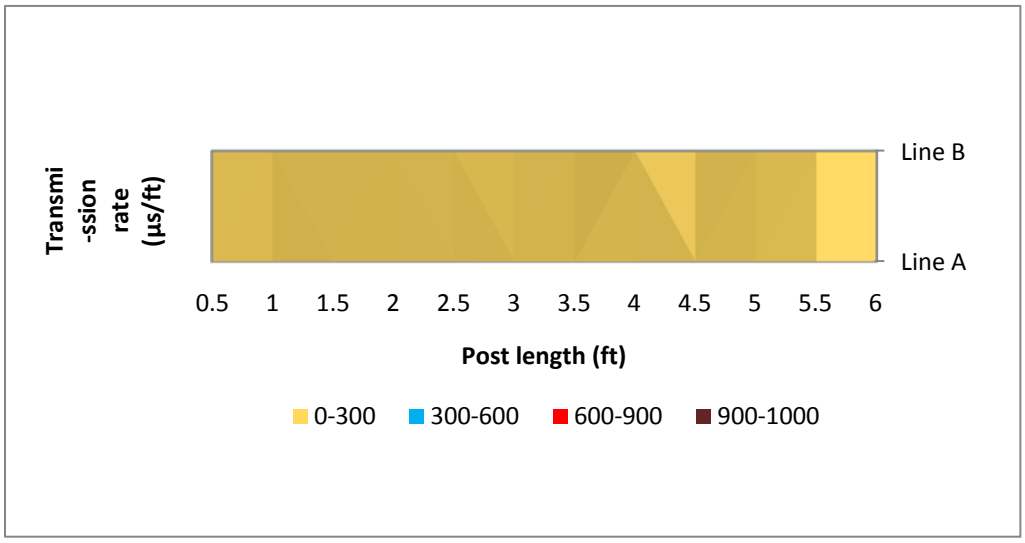

Figure A6. Results from perpendicular-to-grain stress wave scanning for R06 at Royalton site

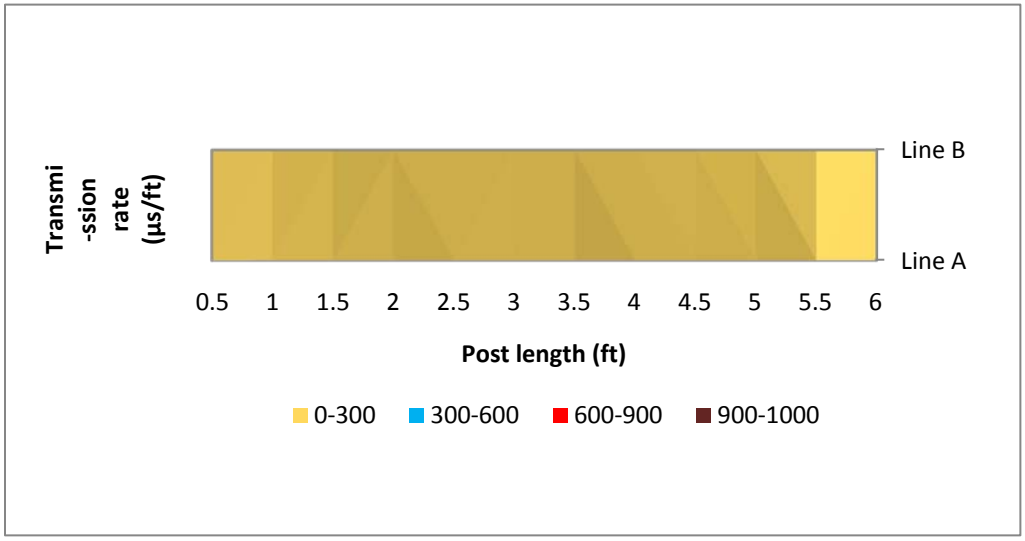

Figure A7. Results from perpendicular-to-grain stress wave scanning for R07 at Royalton site

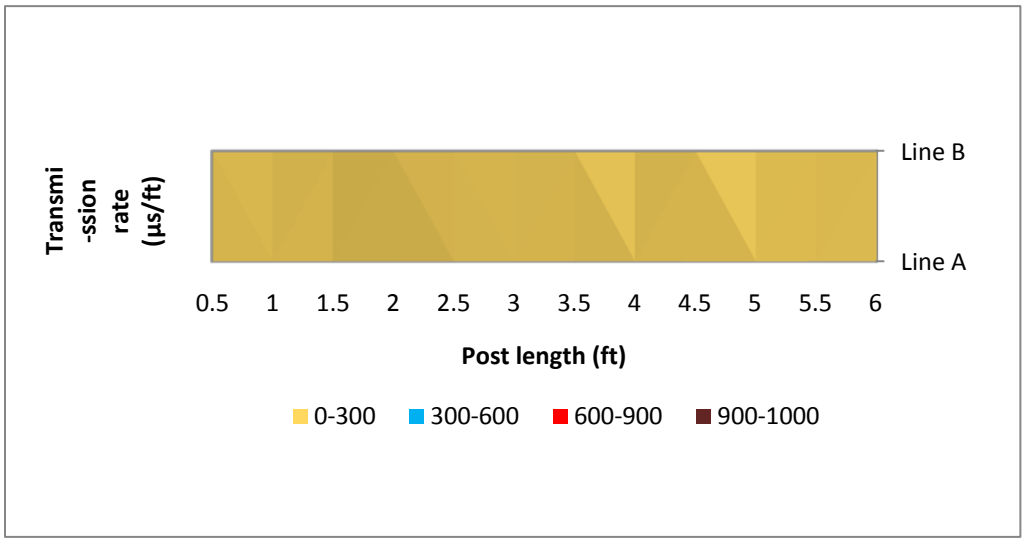

Figure A8. Results from perpendicular-to-grain stress wave scanning for R08 at Royalton site

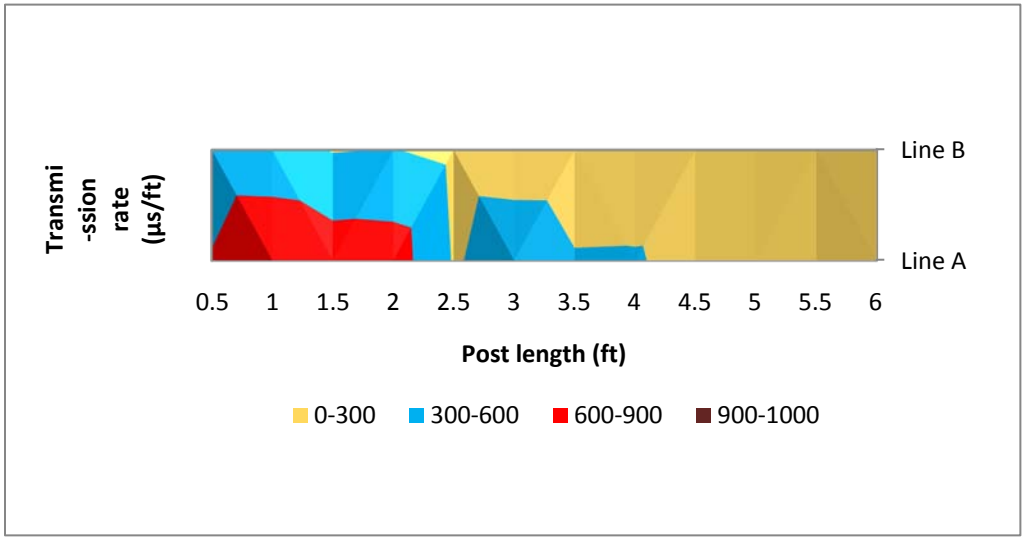

Figure A9. Results from perpendicular-to-grain stress wave scanning for R09 at Royalton site

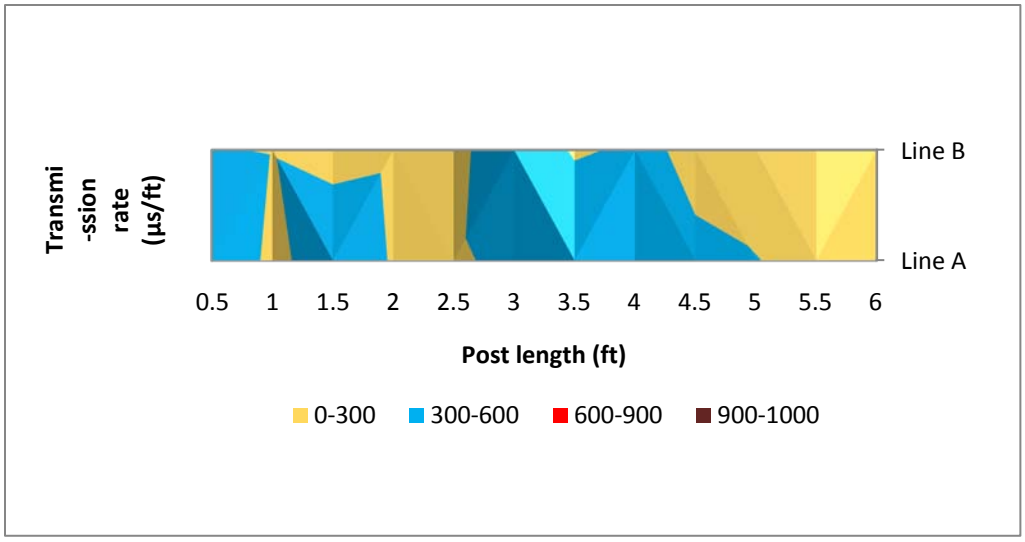

Figure A10. Results from perpendicular-to-grain stress wave scanning for R10 at Royalton site

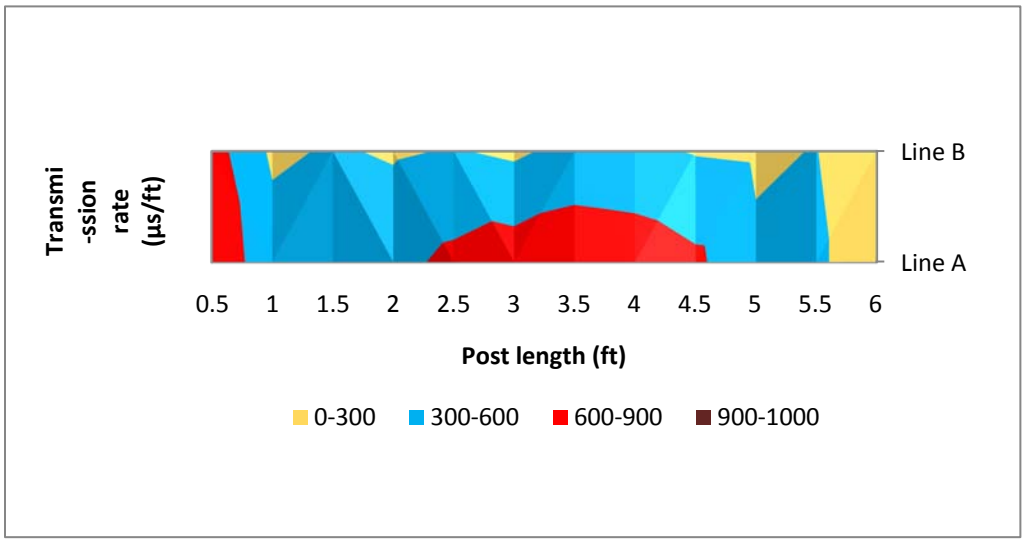

Figure A11. Results from perpendicular-to-grain stress wave scanning for R11 at Royalton site

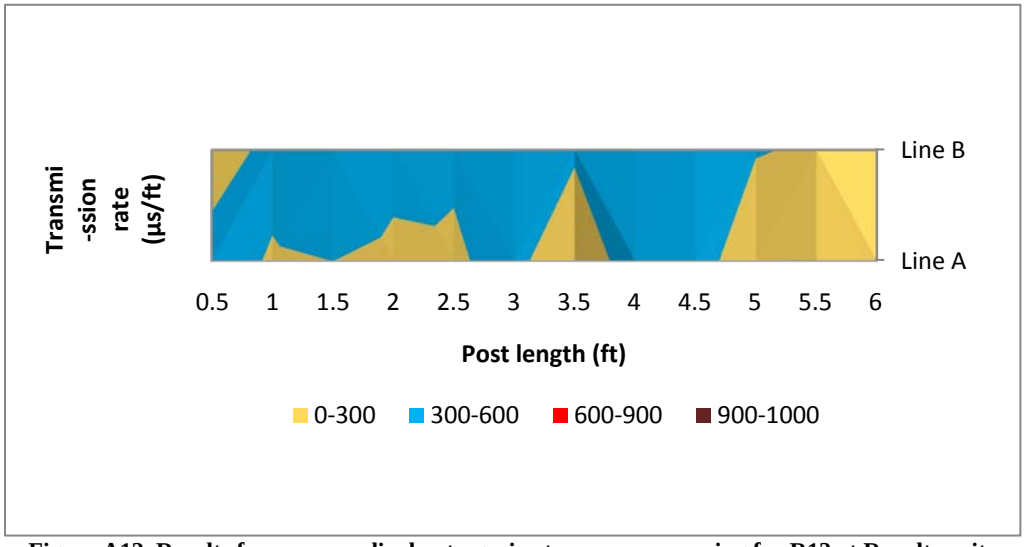

Figure A12. Results from perpendicular-to-grain stress wave scanning for R12 at Royalton site

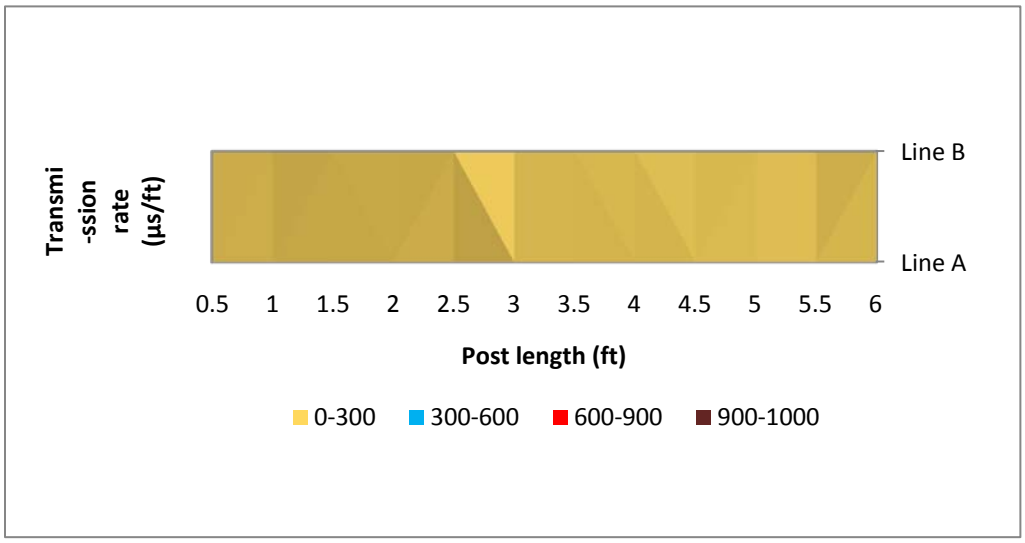

Figure A13. Results from perpendicular-to-grain stress wave scanning for R13 at Royalton site

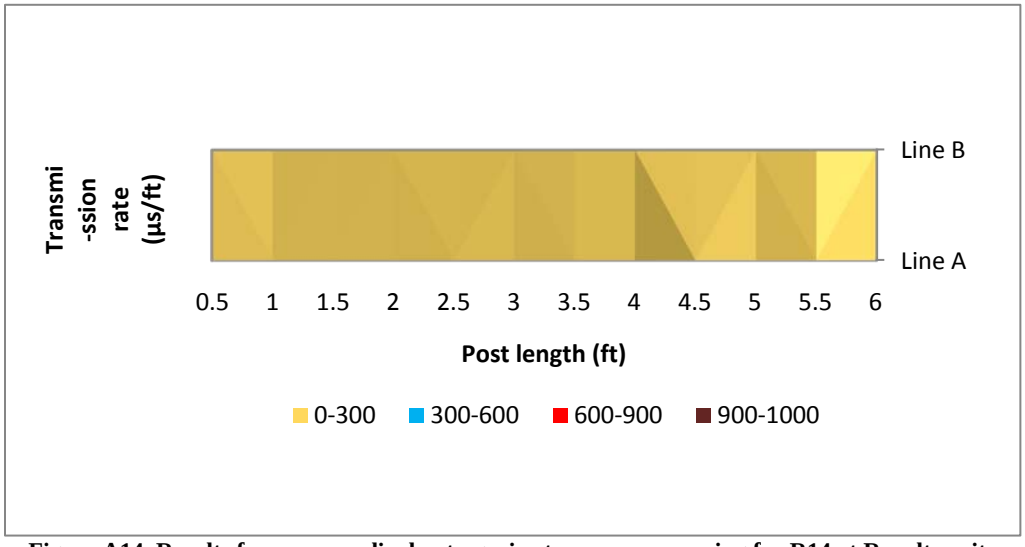

Figure A14. Results from perpendicular-to-grain stress wave scanning for R14 at Royalton site

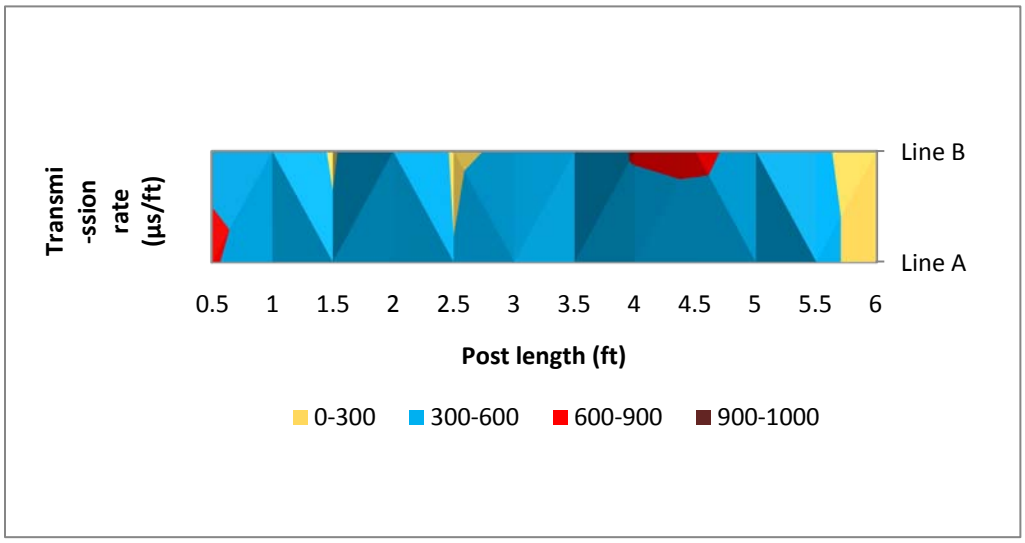

Figure A15. Results from perpendicular-to-grain stress wave scanning for R15 at Royalton site

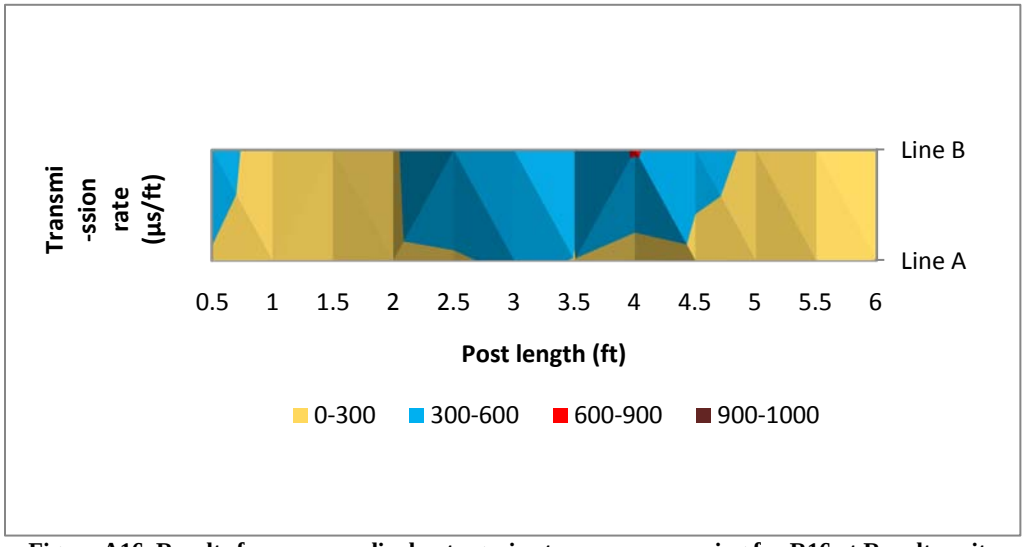

Figure A16. Results from perpendicular-to-grain stress wave scanning for R16 at Royalton site

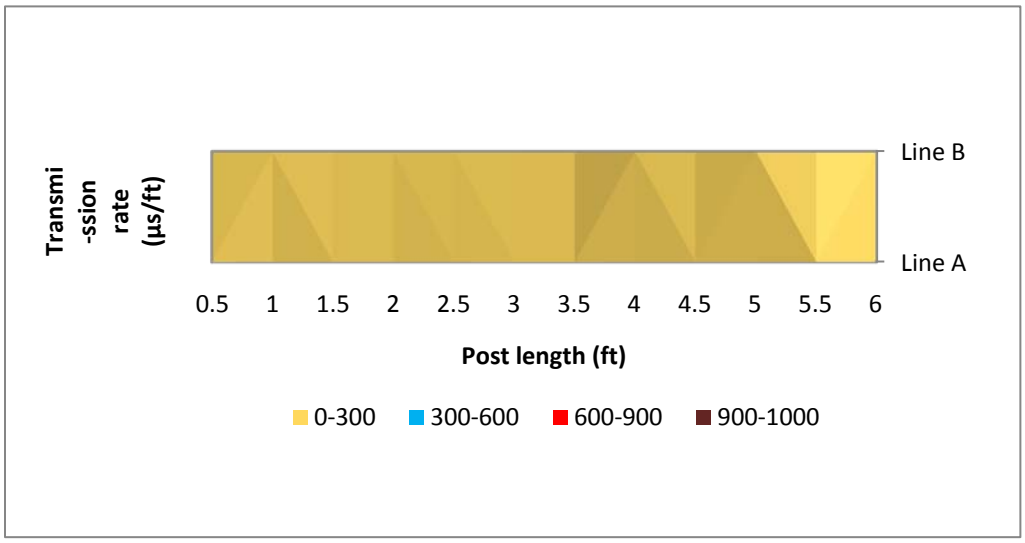

Figure A17. Results from perpendicular-to-grain stress wave scanning for R17 at Royalton site

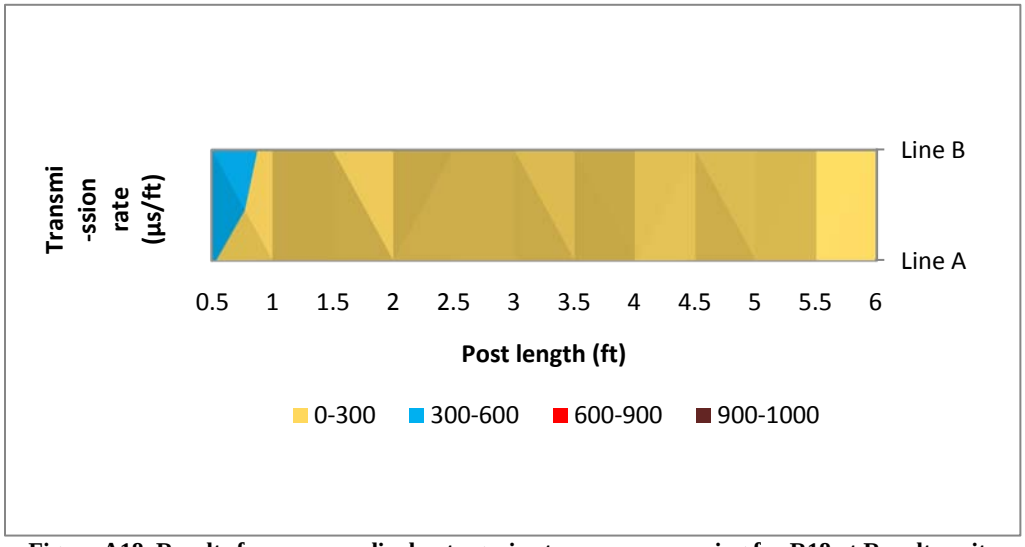

Figure A18. Results from perpendicular-to-grain stress wave scanning for R18 at Royalton site

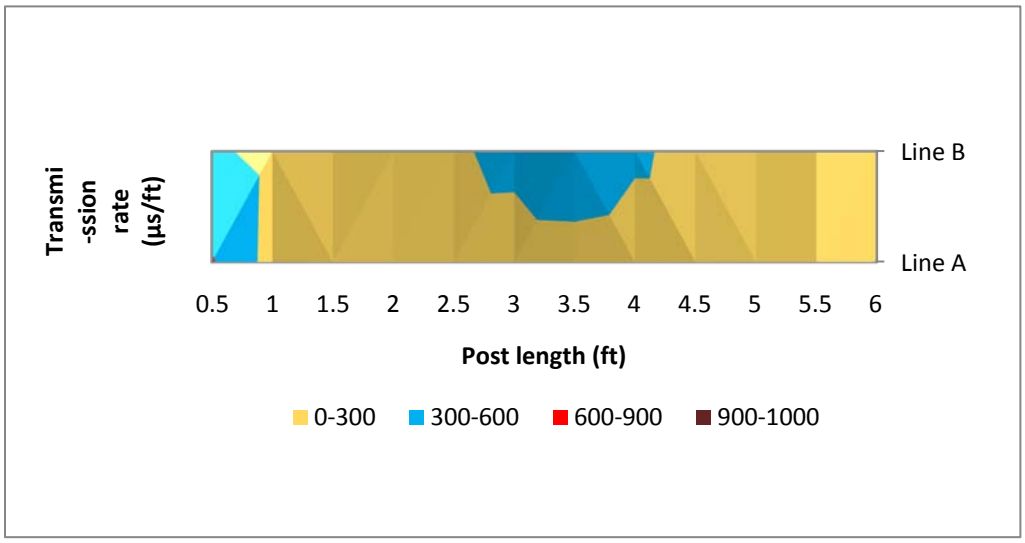

Figure A19. Results from perpendicular-to-grain stress wave scanning for R19 at Royalton site

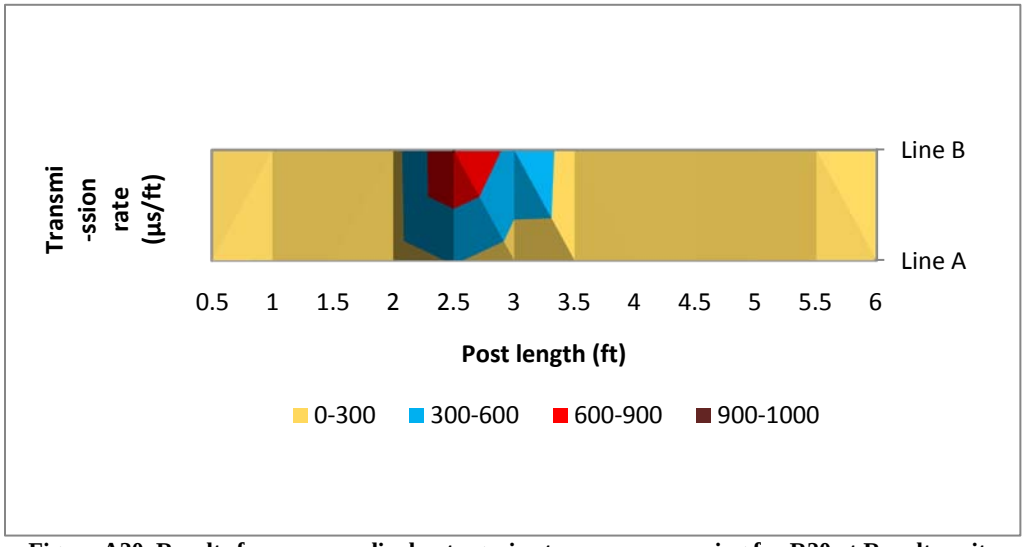

Figure A20. Results from perpendicular-to-grain stress wave scanning for R20 at Royalton site

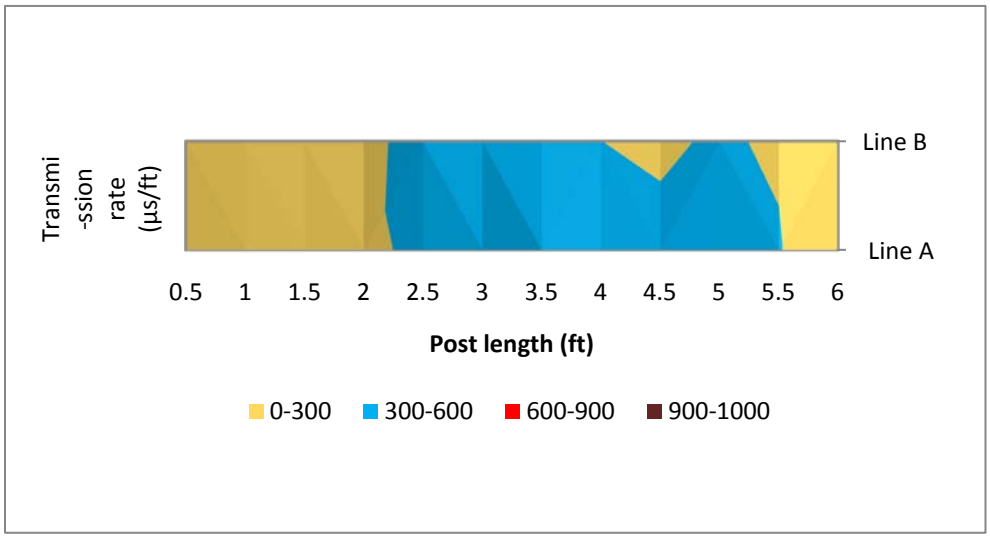

Figure A21. Results from perpendicular-to-grain stress wave scanning for M01 at Merrimac site

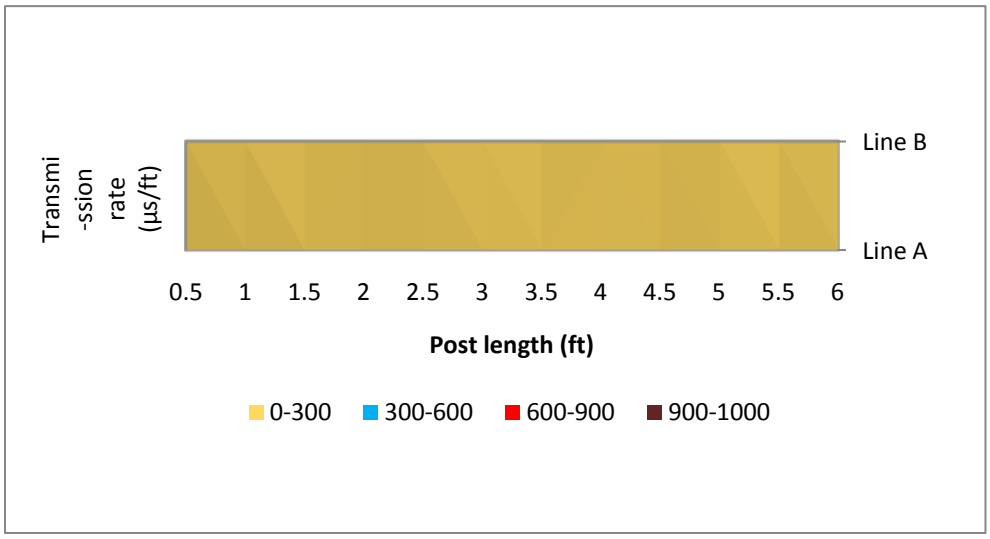

Figure A22. Results from perpendicular-to-grain stress wave scanning for M02 at Merrimac site

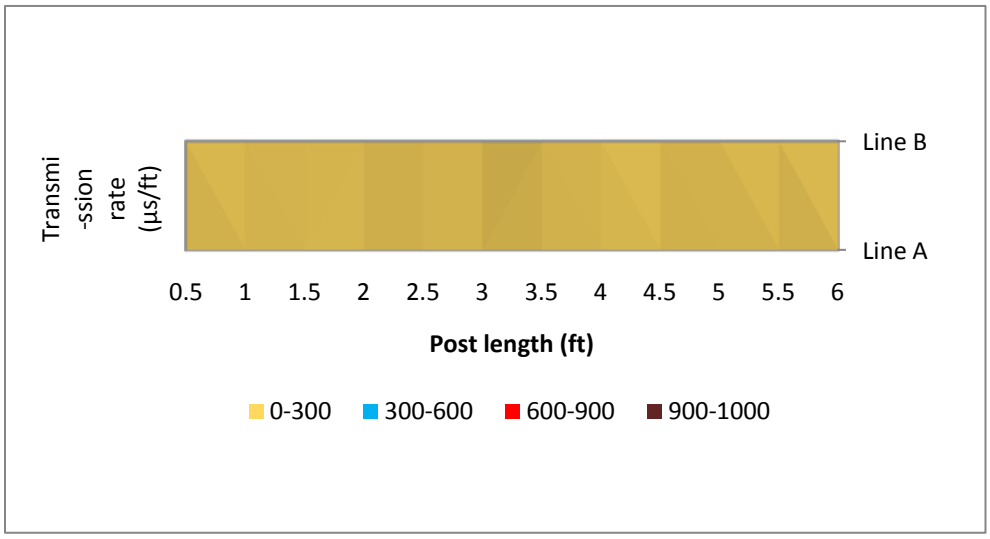

Figure A23. Results from perpendicular-to-grain stress wave scanning for M03 at Merrimac site

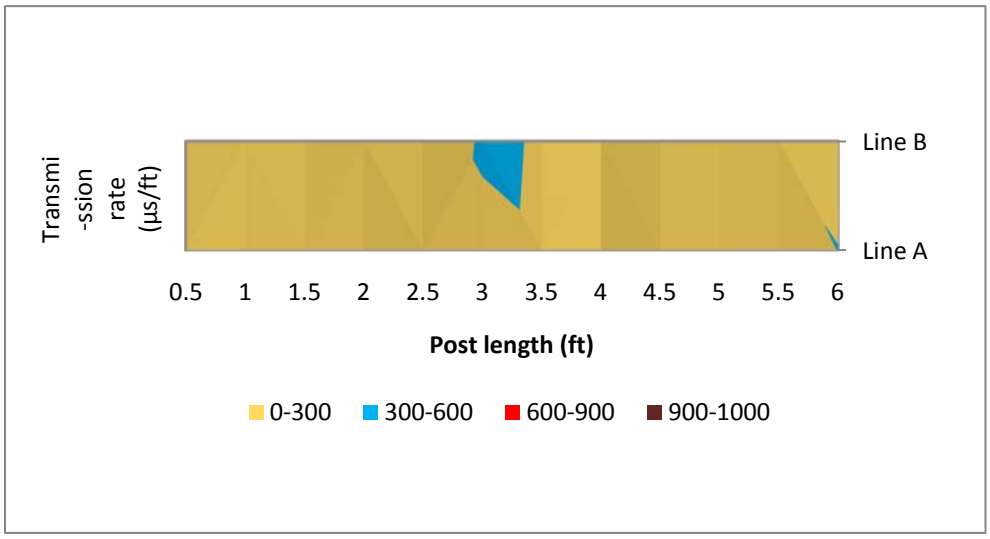

Figure A24. Results from perpendicular-to-grain stress wave scanning for M04 at Merrimac site

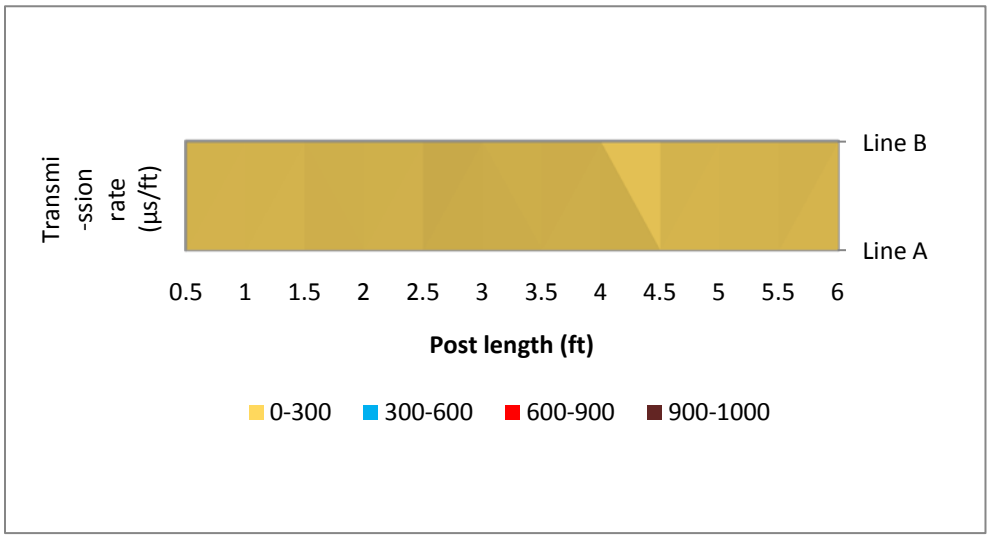

Figure A25. Results from perpendicular-to-grain stress wave scanning for M05 at Merrimac site

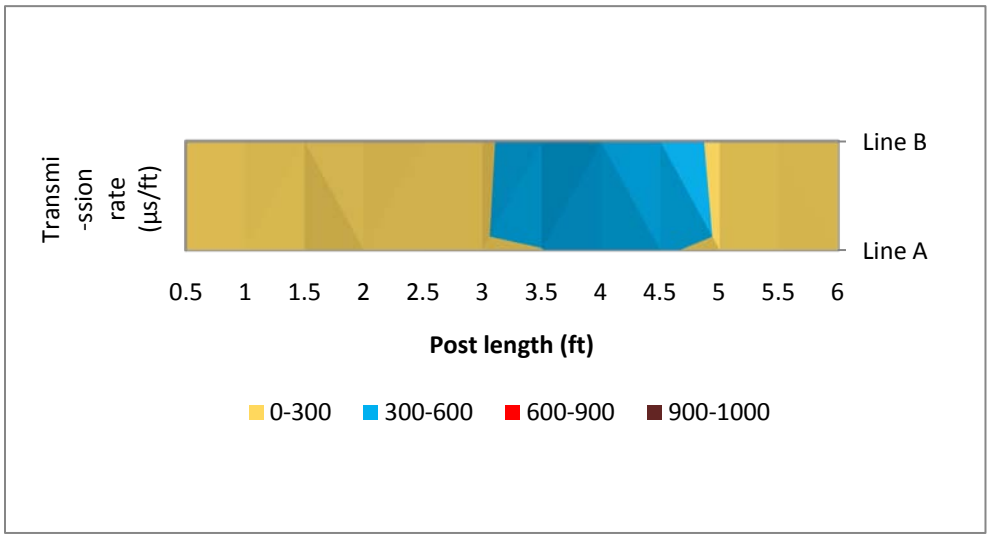

Figure A26. Results from perpendicular-to-grain stress wave scanning for M06 at Merrimac site

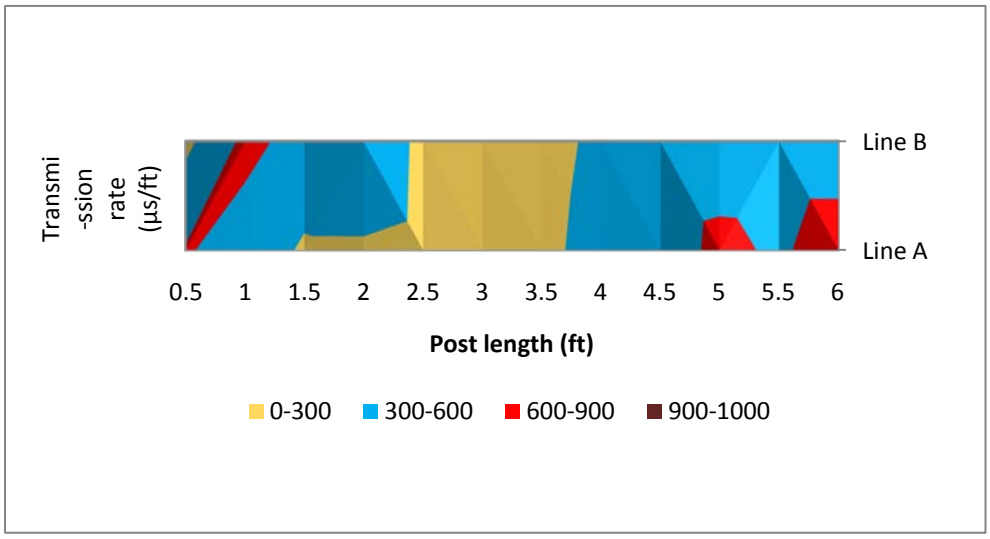

Figure A27. Results from perpendicular-to-grain stress wave scanning for M07 at Merrimac site

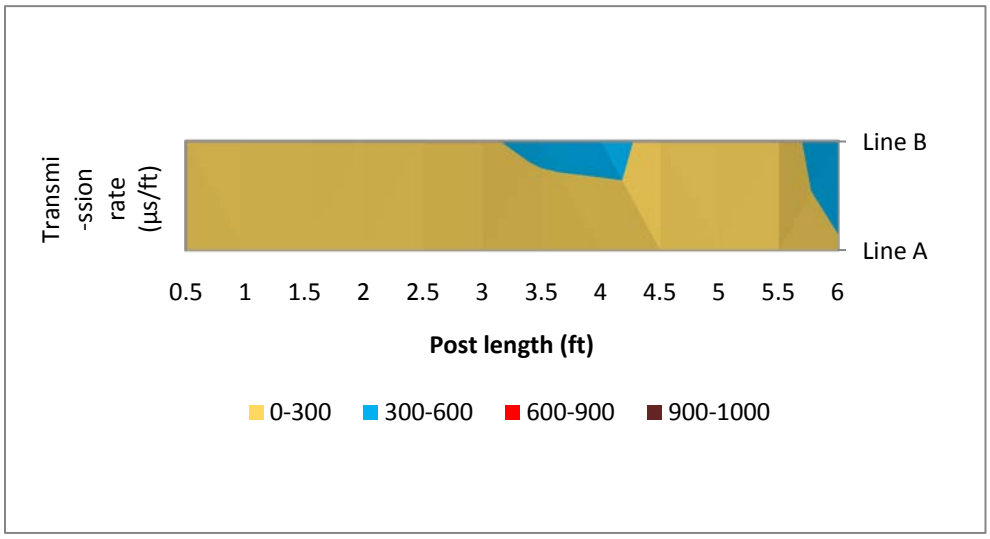

Figure A28. Results from perpendicular-to-grain stress wave scanning for M08 at Merrimac site

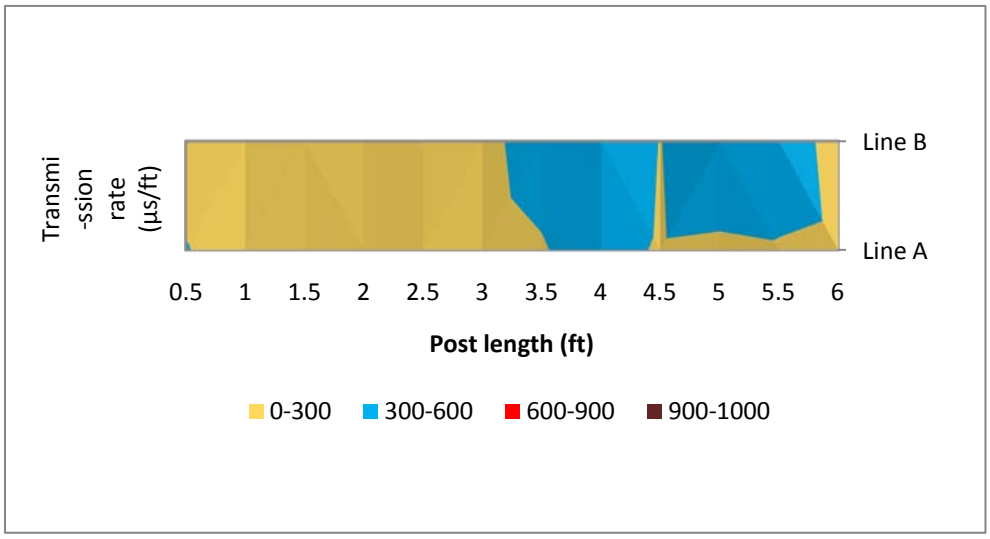

Figure A29. Results from perpendicular-to-grain stress wave scanning for M09 at Merrimac site

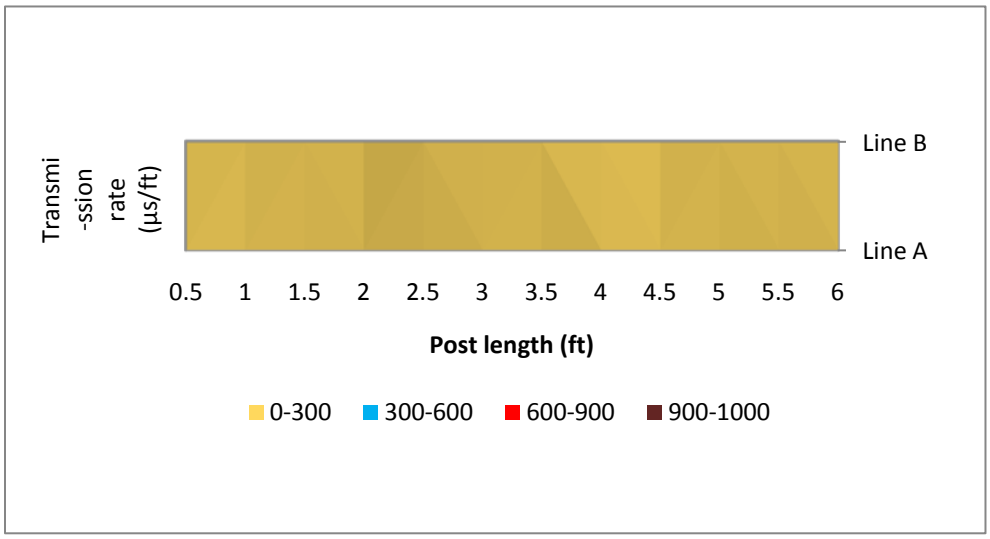

Figure A30. Results from perpendicular-to-grain stress wave scanning for M10 at Merrimac site

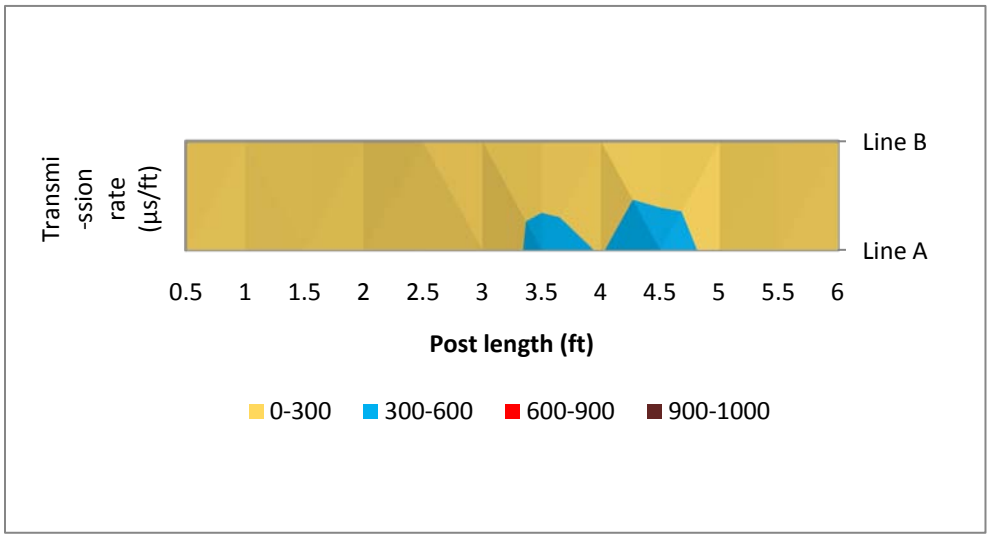

Figure 301. Results from perpendicular-to-grain stress wave scanning for M11 at Merrimac site

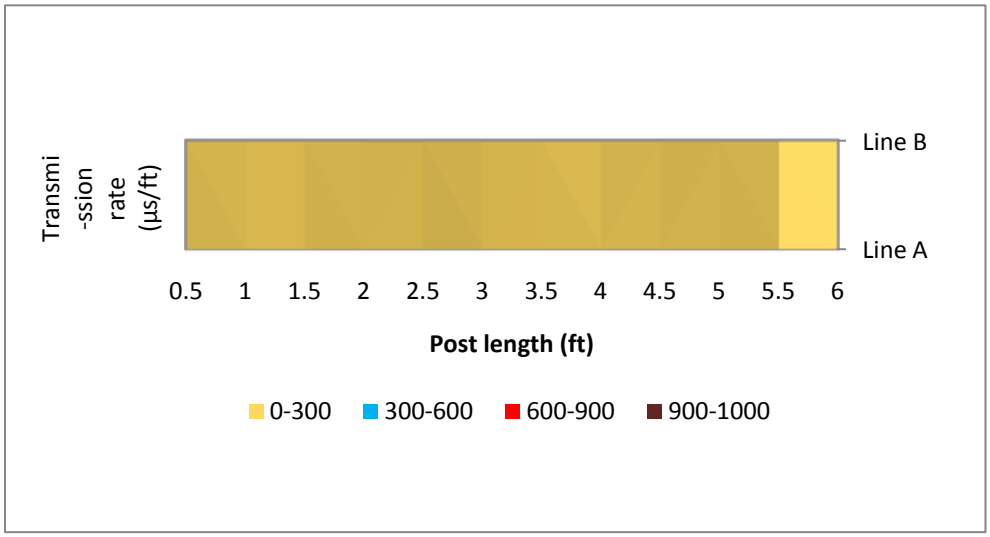

Figure A312. Results from perpendicular-to-grain stress wave scanning for M12 at Merrimac site

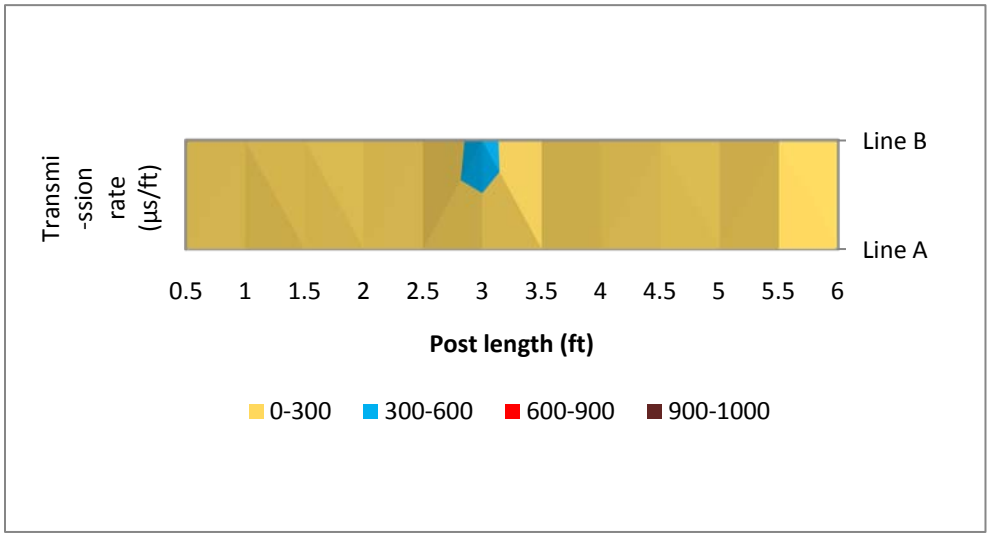

Figure A323. Results from perpendicular-to-grain stress wave scanning for M13 at Merrimac site

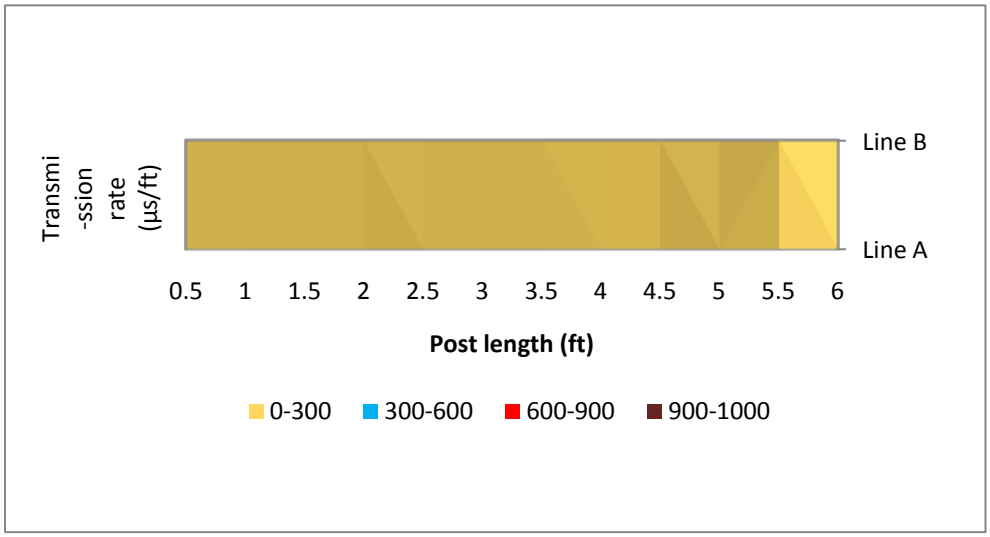

Figure A334. Results from perpendicular-to-grain stress wave scanning for M14 at Merrimac site

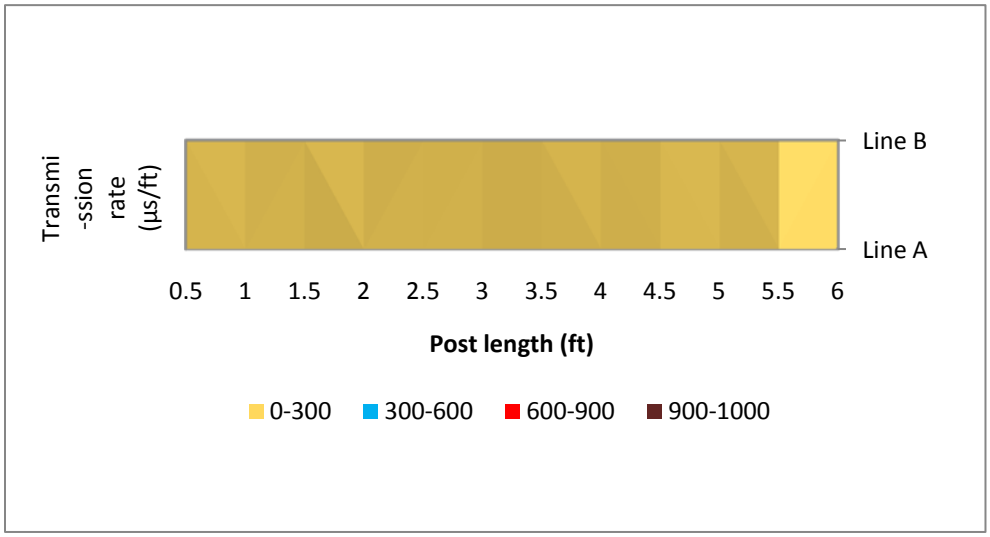

Figure A345. Results from perpendicular-to-grain stress wave scanning for M15 at Merrimac site

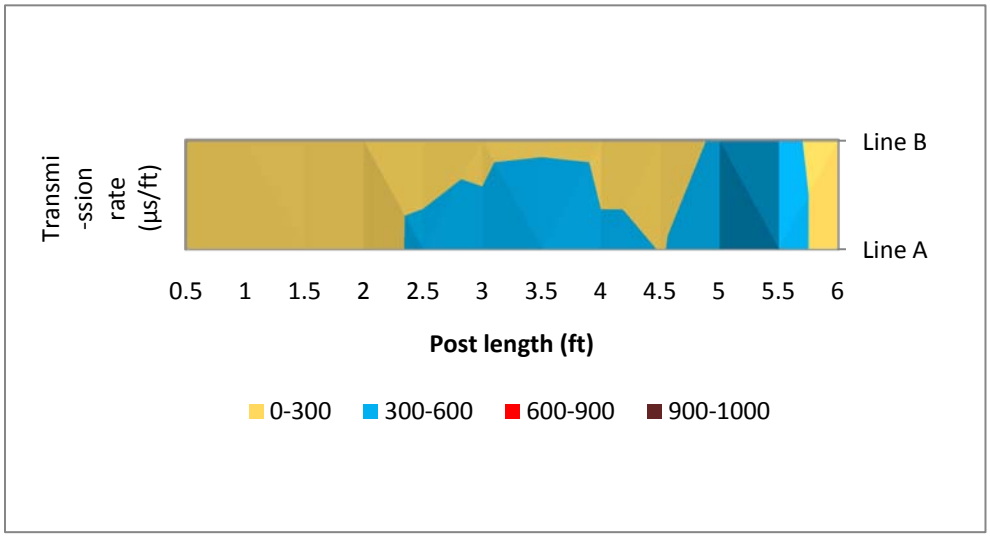

Figure A356. Results from perpendicular-to-grain stress wave scanning for M16 at Merrimac site

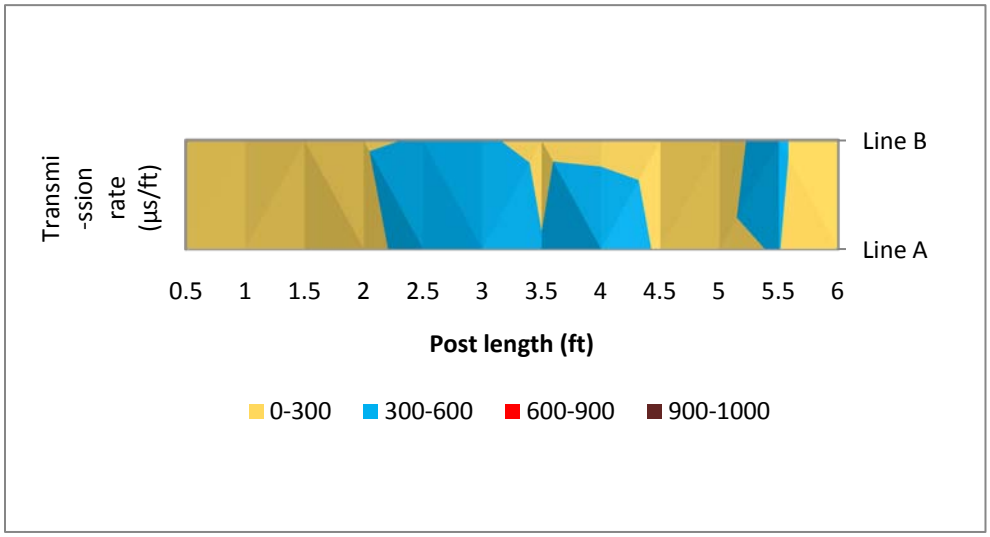

Figure A 367. Results from perpendicular-to-grain stress wave scanning for M17 at Merrimac site

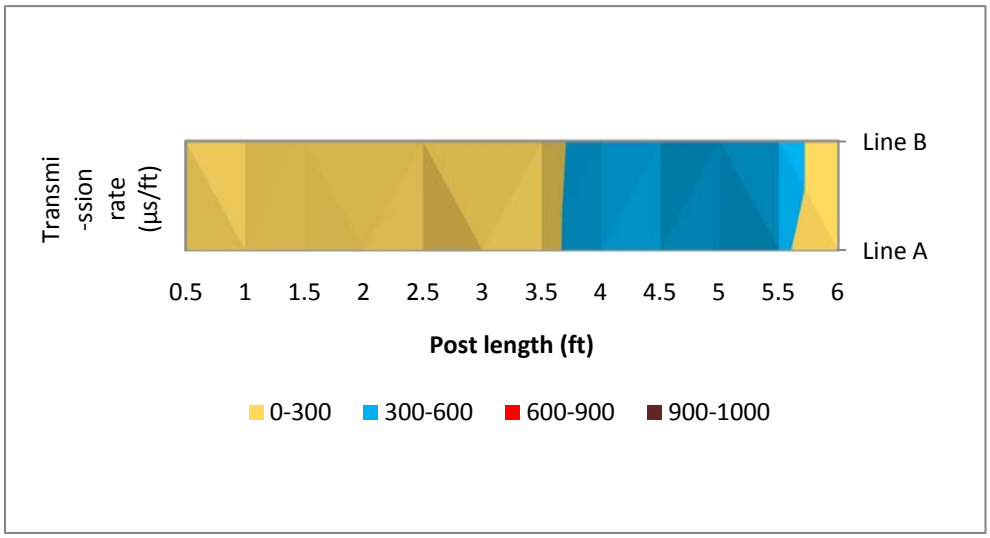

Figure A38. Results from perpendicular-to-grain stress wave scanning for M18 at Merrimac site

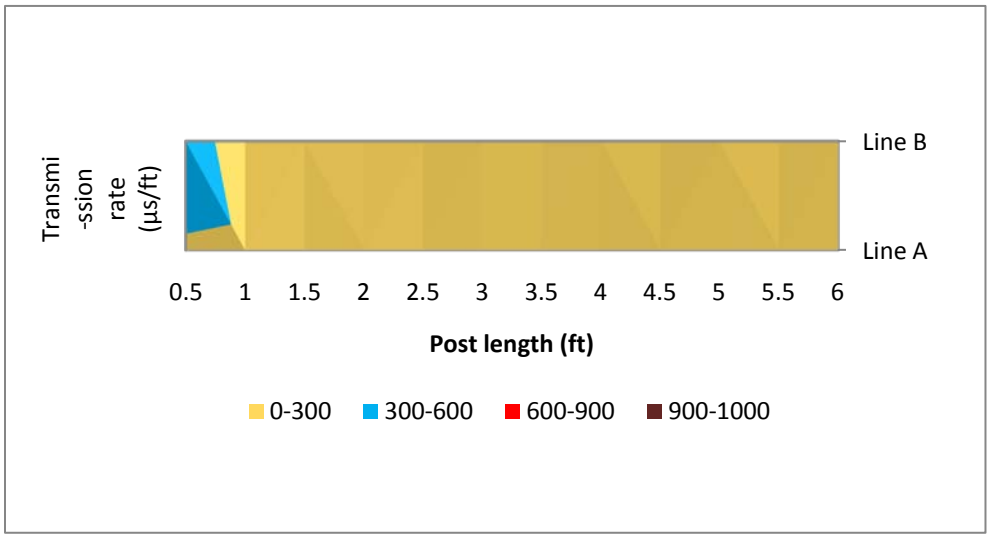

Figure A39. Results from perpendicular-to-grain stress wave scanning for M19 at Merrimac site

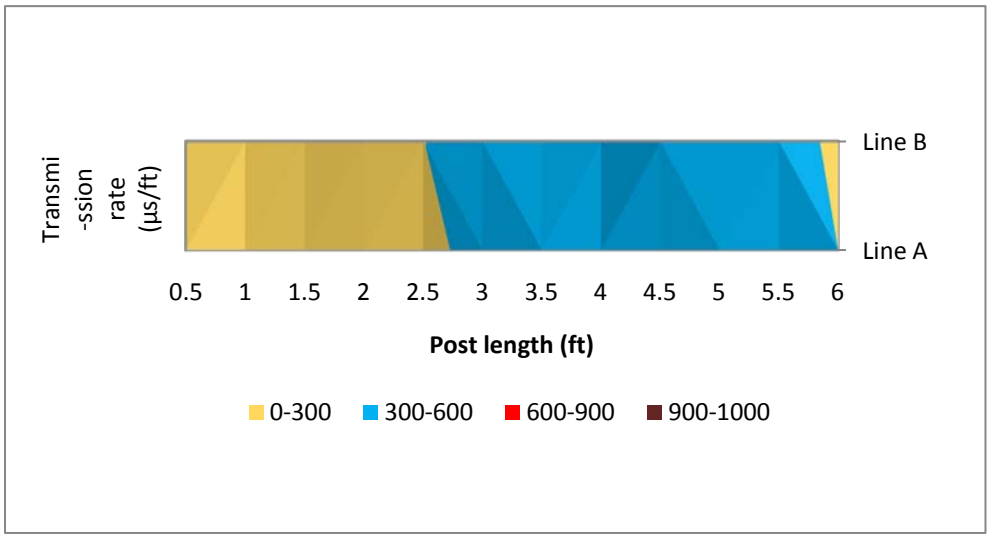

Figure A40. Results from perpendicular-to-grain stress wave scanning for M20 at Merrimac site